# POWER SYSTEM ON-LINE TRANSIENT STABILITY ASSESSMENT

## INTRODUCTION

Recent major blackouts in North America and Europe vividly demonstrated that power interruptions or blackouts can significantly impact the economy and are not acceptable to society. And yet, the ever increasing loading of transmission networks coupled with a steady increase in load demands have pushed the operating conditions of many power systems worldwide ever closer to their stability limits. The combination of limited investment in new transmission and generation facilities, new regulatory requirements for transmission open access, and environmental concerns are forcing transmission networks to carry more power than they were designed to withstand. This problem of reduced operating security margins is being further compounded by factors such as (1) the increasing number of bulk power interchange transactions and non-utility generators, and (2) the trend toward installing higher output generators with lower inertia constants and higher short-circuit ratios. Under these conditions, it is now well recognized that any violation of power system dynamic security limits leads to far-reaching consequences for the entire power system.

By nature, a power system continually experiences two types of disturbances: *event disturbances* and *load variations*. Event disturbances (contingencies) include loss of generating units or transmission components (lines, transformers, substations) from short-circuits caused by lightning, high winds, failures such as incorrect relay operations or insulation breakdown, sudden large load changes, or a combination of such events. Event disturbances usually lead to a change in the network configuration of the power system caused by actions from protective relays and circuit breakers. They can occur in the form of a single equipment (or component) outage or in the form of multiple simultaneous outages when taking relay actions into account. Load variations, on the other hand, are variations in load demands at buses and/or power transfers among buses. The network configuration may remain unchanged after load variations.

Power systems are planned and operated to withstand the occurrence of certain disturbances. The North American Electric Reliability Council defines security as the ability to prevent cascading outages when the bulk power supply is subjected to severe disturbances. The specific criteria that must be met are set by individual reliability councils. Each council establishes the types of disturbances that its system must withstand without cascading outages.

A major activity in power system planning and operations is to examine the impact of a set of credible disturbances on power system dynamic behaviors such as stability. Power system stability analysis is concerned with a power system's ability to reach an acceptable steady state (operating condition) after a disturbance. Stability analysis is one of the most important tasks in power system operations and planning. Today, stability analysis programs are being used by power system planning and operating engineers to simulate the response of the system to various credible disturbances. In these simulations, the dynamic behavior of a current or proposed power system is examined to determine whether stability has been maintained or lost after the contingency. For operational purposes, power system stability analysis plays an important role in determining the system operating limits and operating guidelines. During the planning stage, power system stability analysis is performed to check relay settings, to set the parameters of control devices, or to assess the need for additional facilities and the locations at which to place additional control devices in order to enhance the system's static and dynamic security. Important conclusions and decisions about power system operations and planning are made based on the results of stability studies.

Transient stability problems, a class of power system stability problems, have been a major operating constraint in regions that rely on long-distance transfers of bulk power (e.g., in most parts of the Western Interconnection of the United States., Hydro Quebec, the interfaces between Ontario and the New York area and the Manitoba/Minnesota area, and in certain parts of China and Brazil). The trend now, with increased instances and total volume of bulk power transfer, is that many parts of the various interconnected systems are becoming constrained by transient stability limitations. The wave of recent changes has greatly increased the adverse effect of both event disturbances and load variations on power system stability. Hence, it is imperative to develop powerful tools to examine power system stability in a timely and accurate manner and to derive necessary control actions for both preventive control and enhancement control.

On-line transient stability assessment (TSA) is an essential tool needed to avoid any violation of dynamic security limits. Indeed, with current power system operating environments, it is increasingly difficult for power system operators to generate all operating limits for all possible operating conditions under a list of credible contingencies. Hence, it is imperative to develop a reliable and effective on-line TSA to obtain the operating security limits at or near real time. In addition to this important function, power system transmission open access and restructuring further reinforce the need for an on-line TSA as it is the base upon which determination of available transfer capability and dynamic congestion management problems and coordination of special protection systems can be effectively resolved.

Significant engineering and financial benefits are expected from an on-line TSA. First, one may be able to operate a power system with operating margins reduced by a factor of 10 or more if the transient stability assessment is based on the actual system configuration and operating conditions, instead of assumed worst-case conditions, as is done in off-line studies. A second benefit of on-line analysis is that the analysis can be reduced to those cases relevant to actual operating conditions, thereby obtaining more accurate operating margins, allowing more power transfer, and freeing engineering resources for other critical activities.

J. Webster (ed.), *Wiley Encyclopedia of Electrical and Electronics Engineering*. 

Modern energy management systems periodically perform the tasks of on-line power system static security assessment and control for ensuring the ability of the power system to withstand a set of credible contingencies (disturbances). The assessment involves the selection of the set of credible contingencies and then the evaluation of the system's response to contingencies. Various software packages for security assessment and control have been implemented in modern energy control centers. These packages provide comprehensive on-line security analysis and control based almost exclusively on steady-state analysis, making them applicable only to static security assessment and control [1].

From a computational viewpoint, on-line TSA requires the handling of a large set of mathematical models, which is described by a large set of nonlinear differential equations in addition to the nonlinear algebraic equations involved in the static security assessment. The computational effort required by on-line TSA is roughly three magnitudes higher than that for the static security assessment (SSA). This result explains why TSA has long remained an off-line activity instead of on-line activity in the energy management system. Extending the functions of energy management systems to take account of on-line TSA and control is a rather challenging task and requires several breakthroughs in measurement systems, analysis tools, computation methods, and control schemes.

Currently, stability analysis programs routinely used in utilities around the world are based mostly on step-by-step numerical integrations of power system stability models to simulate system dynamical behaviors. This practice of power system stability analysis based on the time-domain approach has a long history [1–12]. However, because of the nature of the time-domain approach, it has several disadvantages: (1) It requires intensive, time-consuming computation efforts; therefore, it has not been suitable for on-line application; (2) it does not provide information as to how to derive preventive control when the system is deemed unstable and how to derive enhancement control when the system is deemed critically stable; and (3) it does not provide information regarding the degree of stability (when the system is stable) and the degree of instability (when the system is unstable). This piece of information is valuable for both planning and operations.

An alternative approach to transient stability analysis employing energy functions, called *direct methods*, was originally proposed by Magnusson [13] in the late 1940s and was pursued in the 1950s by Aylett [14]. Direct methods have a long development history spanning six decades. Significant progress, however, has been made recently in the practical application of direct methods to transient stability analysis. Direct methods can determine transient stability without the time-consuming numerical integration of the (post-fault) power system [15–18]. In addition to its speed, direct methods also provide a quantitative measure of the degree of system stability. This additional information makes direct methods very attractive when the relative stability of different network configuration plans must be compared or when system operating limits constrained by transient stability must be calculated quickly. Another advantage of direct methods is the ability to provide useful information regarding how to derive preventive control actions when the underlying power system is deemed unstable and how to derive enhancement control actions when the underlying power system is deemed critically stable.

After decades of research and developments in the energy-function-based direct methods and the time-domain simulation approach, it has become clear that the capabilities of direct methods and that of the time-domain approach complement each other. The current direction of development is to include appropriate direct methods and time-domain simulation programs within the body of overall power system stability simulation programs [19–22]. For example, the direct method provides the advantages of fast computational speed and energy margins, which make it a good complement to the traditional time-domain approach. The energy margin and its functional relations to certain power system parameters are an effective complement to develop tools such as preventive control schemes for credible contingencies that are unstable and to develop fast calculators for available transfer capability limited by transient stability. The direct method can also play an important role in the dynamic contingency screening for on-line transient stability assessment.

## PROBLEM FORMULATION AND SYSTEM MODEL

Electric power systems are nonlinear in nature. Their nonlinear behaviors are difficult to predict because of (1) the extraordinary size of the systems, (2) the nonlinearity in the systems, (3) the dynamical interactions within the systems, and (4) the complexity of its component modeling. These complicating factors have forced power system engineers to analyze the complicated behaviors of power systems through the process of modeling, simulation and validation.

The complete power system model for calculating system dynamic response relative to a disturbance comprises a set of first-order differential equations

$$\dot{x} = f(x, y, u) \tag{1}$$

describing the internal dynamics of devices such as generators, their associated control systems, certain loads and other dynamically modeled components, and a set of algebraic equations

$$0 = g(x, y, u) \tag{2}$$

describing the electrical transmission system (the interconnections between the dynamic devices) and internal static behaviors of passive devices (such as static loads, shunt capacitors, fixed transformers, and phase shifters). The differential equations (1) typically describe the dynamics of the speed and angle of generator rotors; the flux behaviors in generators; the response of generator control systems such as excitation systems, voltage regulators, turbines, governors, and boilers; the dynamics of equipment such as synchronous VAR compensators (SVCs), DC lines, and their control systems; and the dynamics of dynamically modeled loads such as induction motors. The stated variables $x$ typically include generator rotor

angles, generator velocity deviations (speeds), mechanical powers, field voltages, power system stabilizer signals, various control system internal variables, and voltages and angles at load buses (if dynamic load models are employed at these buses). The algebraic equations (2) comprise the stator equations of each generator, the network equations of transmission networks and loads, and the equations defining the feed-back stator quantities. An aggregated representation of each local distribution network is usually used in simulating power system dynamical behaviors. The forcing functions $u$ acting on the differential equations are terminal voltage magnitudes, generator electrical powers, and signals from boilers and automatic generation control systems.

Some control system internal variables have upper bounds on their values because of their physical saturation effects. Let $z$ be the vector of these constrained state variables; then the saturation effects can be expressed as

$$0 < z(t) \leq \bar{z} \tag{3}$$

A detailed description of equations (1)–(3) for each component can be found, for example, in Refs. 3 and 4. For a 900-generator, 14,000-bus power system, the number of differential equations can easily reach as many as 20,000, whereas the number of nonlinear algebraic equations can easily reach as many as 32,000. The sets of differential equations (1) are usually loosely coupled.

To protect power systems from damage caused by disturbances, protective relays are placed strategically throughout a power system to detect faults (disturbances) and to trigger the opening of circuit breakers necessary to isolate faults. These relays are designed to detect defective lines and apparatus or other power system conditions of an abnormal or dangerous nature and to initiate appropriate control circuit actions. Because of the action of these protective relays, a power system subject to an event disturbance can be viewed as going through changes in its network configuration in three stages: from the pre-fault, to the fault-on, and finally to the post-fault system. The pre-fault system is in a stable steady state; when an event disturbance occurs, the system then moves into the fault-on system before it is cleared by protective system operations. Stated more formally, in the pre-fault regime, the system is at a known stable equilibrium point (SEP), say $(x_s^{\text{pre}}, y_s^{\text{pre}})$. At some time $t_0$ the system undergoes a fault (an event disturbance), which results in a structural change in the system caused by actions from relay and circuit breakers. Suppose the fault duration is confined to the time interval $[t_0, t_{cl}]$. During this interval, the fault-on system is described by (for ease of exposition, the saturation effects expressed as $0 < z(t) \leq \bar{z}$ are neglected in the following):

$$\begin{aligned} \dot{x} &= f_F(x, y) \quad t_0 \leq t < t_{cl} \\ 0 &= g_F(x, y) \end{aligned} \tag{4}$$

where $x(t)$ is the vector of state variables of the system at time $t$. Sometimes, the fault-on system may involve more than one action from system relays and circuit breakers. In these cases, the fault-on systems are described by several

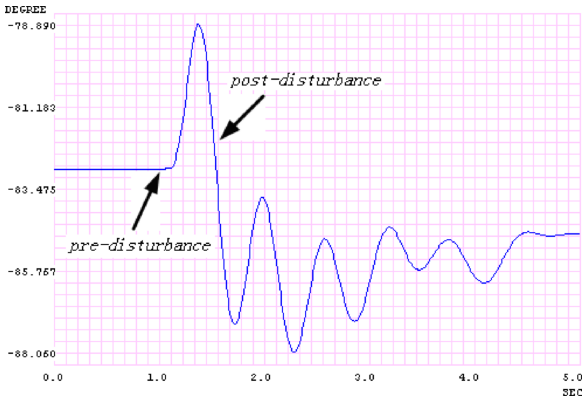


**Figure 1.** The simulated dynamical behavior, pre-fault, fault-on, and post-fault of a generator's angle of a large power system model.

sets of nonlinear equations:

$$\begin{aligned} \dot{x} &= f_F^1(x, y), \quad t_0 \leq t \leq t_{F,1} \\ 0 &= g_F^1(x, y) \\ \dot{x} &= f_F^k(x, y), \quad t_{F,1} \leq t \leq t_{F,2} \\ 0 &= g_F^2(x, y) \\ &\cdots \\ \dot{x} &= f_F^k(x, y), \quad t_{F,k} \leq t \leq t_{cl} \\ 0 &= g_F^k(x, y) \end{aligned} \tag{5}$$

The number of sets of equations equals the number of separate actions from system relays and circuit breakers. Each set depicts the system dynamics caused by one action from relays and circuit breakers. Suppose the fault is cleared at time $t_{cl}$ and no additional protective actions occur after $t_{cl}$. The system, termed the post-fault system, is henceforth governed by post-fault dynamics described by

$$\begin{aligned} \dot{x} &= f_{PF}(x, y), t_{cl} \leq t < \infty \\ 0 &= g_{PF}(x, y) \end{aligned} \tag{6}$$

The network configuration may or may not be the same as the pre-fault configuration in the post-fault system. We will use the notation $z(t_{cl}) = (x(t_{cl}), y(t_{cl}))$ to denote the fault-on state at switching time $t_{cl}$ The post-fault trajectory after an event disturbance corresponds to the solution of equation (5) over the fault-on time period $t_0 \leq t < t_{cl}$ and the solution of equation (6) over the post-fault time period $t_{cl} \leq t < t_\infty$.

The fundamental problem of power system stability caused by a fault (i.e., a contingency) can be roughly stated as follows: Given a pre-fault SEP and a fault-on system, will the post-fault trajectory settle down to an acceptable steady state [18]? A simulated system trajectory starting from a pre-fault SEP, fault-on trajectory and post-fault trajectory, is shown in Figs. 1 and 2.

The two sets of equations (1) and (2) describing power system dynamic response relative to a contingency are fairly complex, because electric power systems comprise a large number of components (equipment and control devices) interacting with each other, exhibiting nonlinear dynamic behaviors with a wide range of time scales. The dynamic behavior after a disturbance involves all system components, to varying degrees. The degree of involvement from each component determines the appropriate system model necessary for simulating the dynamic behaviors. Traditional practice in power system analysis has been to

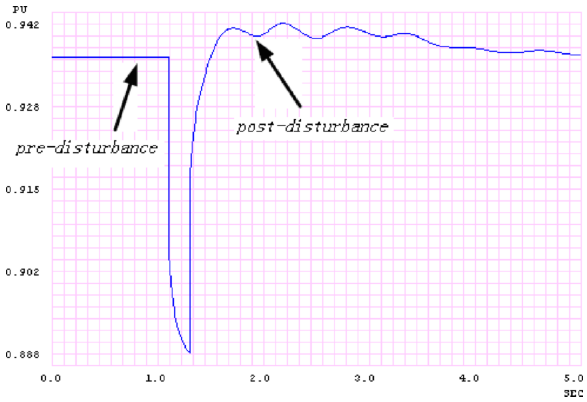


**Figure 2.** The simulated dynamical behavior, pre-fault, fault-on, and post-fault of a voltage magnitude of a large power system model. During the fault, the voltage magnitude drops to about 0.888 p.u.

use the simplest acceptable system model that captures the essence of the phenomenon under study. A logic commonly used in power system dynamic simulations is that the effect of a system component or control device can be neglected when the time scale of its response is very small or very large compared with the time period of interest and, hence, can be considered in quasi-steady state. This philosophy has been deemed acceptable because of the severe complexity involved with a full large-scale power system model.

Based on the different time-scale involvement of each component and control device on the overall system dynamic behaviors, power system models have been divided into three models with different time scales: (1) short-term stability model (predominately describing electromechanical transients) on which transient stability is based, (2) extended transient and mid-term stability model, and (3) long-term stability model on which long-term stability is based. These three models are described by a set of differential-algebraic equations of the same nature as equations (1) and (2) but with different sets of state variables with different time constants. However, a "fuzzy" boundary distinguishes between the mid-term and long-term model. Compared with transient stability analysis, mid-term and long-term dynamic behaviors have only come under study relatively recently [3,4,23]. For transient stability analysis, the assumption of one unique frequency is kept for the transmission network model, but generators have different speeds. Generators are modeled in greater detail, with shorter time constants compared with the models used in long-term stability analysis. Roughly speaking, transient stability models reflect the fast-varying system electrical components and machine angles and frequencies, whereas the long-term models are concerned with the representation of the slow oscillatory power balance, assuming that the rapid electrical transients have damped out.

## ON-LINE TSA

On-line TSA is designed to provide system operators with critical information, including, (1) the transient stability of the system subject to a list of contingencies and (2) available (power) transfer limits at key interfaces subject to transient stability constraints. An integrated architecture for on-line TSA and control is presented in Fig. 3. In this architecture, there are two major components in the on-line TSA module: dynamic contingency screening and a fast time-domain stability program for performing detailed stability analysis. Several systems have been developed intended for on-line TSA [24–29].

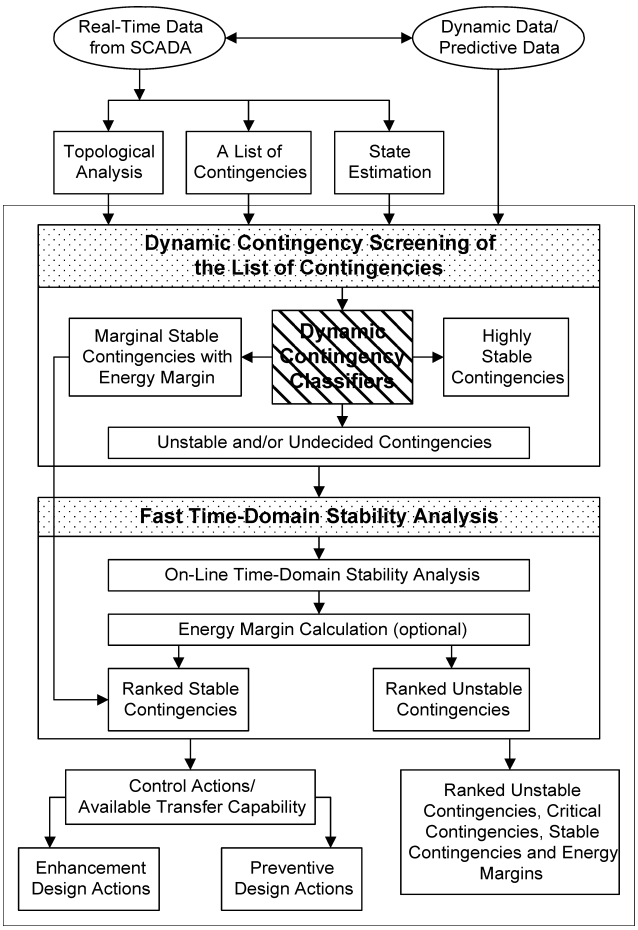


**Figure 3.** An architecture for on-line transient stability assessment and control.

When a new cycle of TSA is warranted, a list of credible contingencies, along with information from the state estimator and topological analysis, are applied to the dynamic contingency screening program whose basic function is to screen out contingencies that are definitely stable or potentially unstable. Contingencies that are classified to be definitely stable are eliminated from additional analysis. Contingencies that are classified to be potentially unstable are sent to fast time-domain simulation for detailed analysis. It is the ability to perform dynamic contingency screening on a large number of contingencies and to filter out a much smaller number of contingencies requiring additional analysis that makes on-line TSA feasible. Contingencies that are either undecided or identified as unstable are then sent to the time-domain transient stability simulation program for detailed stability analysis.

The block function of control actions decisions determines whether timely post-fault contingency corrective

actions such as automated remedial actions are feasible to steer the system from unacceptable conditions to an acceptable state. If appropriate corrective actions are not available, the block function of preventive actions determines the required pre-contingency preventive controls such as real power redispatches or line switching to maintain the system stability should the contingency occur. If the system will be marginally stable; i.e., critically stable, the block function of enhancement actions determines the required pre-contingency enhancement controls such as real power redispatches or line switching to increase the degree of system stability should the contingency occur. In this architecture, a fast and yet reliable method for performing dynamic contingency screening plays a vital role in the overall process of on-line TSA.

Two types of basic information are needed to perform power system on-line TSA: static data (which is the power flow data) and dynamic data. The power flow data describe the network and its steady-state operating conditions, which corresponds to a real-time system condition captured by the EMS and solved by state estimators. The dynamic data supply the information needed to compute the response of the modeled devices to a given disturbance, which refers to dynamic models and data matching the real-time power flow. The dynamic data include models of detailed synchronous machines, dynamic load models, induction motor, static VAR compensator, high-voltage DC link, FACTS, and user-defined models. Another set of data, sequence network data, is required only if unbalanced faults are to be simulated. This set of data contains the negative and zero sequence network data compatible with power flow data.

In addition to the above basic information, the following additional information is needed:

- Description of disturbances: this information describes the disturbance to be simulated, e.g., fault location and duration, circuit switching, or generation/load rejection.
- Relay data: These data describe the characteristics of the protection devices.

A complete on-line TSA assessment cycle will be completed within, say, 15 minutes. This cycle starts when all necessary data are available to the system and ends when the system is ready for the next cycle. Depending on the size of the underlying power system, it is estimated that, for a large-size power system such as 15,000-bus power system, the number of contingencies in a contingency list is between 1000 and 3000. The contingency types will include both three-phase faults with primary clearance and single-line-to-ground faults with backup clearance.

The outputs of on-line TSA in a given cycle include the following:

- Overall status of the system (secure or insecure and the operating margin).
- Unstable contingencies (contingency details such as fault type, fault location, and circuits lost).
- Stability margin in terms of energy margin, or operating margin in MW and/or MVar for each unstable contingency and may include preventive control actions.
- Detailed time-domain responses (swing curves) of user-specified quantities for potentially unstable contingencies.
- Critical contingencies (contingency details such as fault type, fault location, and circuits lost).
- Stability margin in terms of energy margin, or operating margin in MW and/or MVar for each critical contingency and may include enhancement control actions.
- Detailed time-domain responses (swing curves) of user-specified quantities for critical contingencies.
- If transfer limits are computed, limits (or security boundary) at key interfaces, and the limiting contingencies.

In addition to the above main functions, the on-line TSA system should have the following functions:

- A study mode with which the users, such as reliability engineers, can analyze various scenarios using cases archived from real-time system models or created from operational planning studies.
- Software and hardware failover protection.
- Interfaces with EMS functions.
- Definition of contingency list and creation of necessary data for stability analysis, data validation and correction (option), and output visualization.

## DYNAMIC CONTINGENCY SCREENING

The strategy of using an effective scheme to screen out a large number of stable contingencies and capture critical contingencies and to apply detailed simulation programs only to potentially unstable contingencies is well recognized. This strategy has been successfully implemented in on-line SSA. The ability to screen several hundred contingencies to capture tens of the critical contingencies has made the on-line SSA feasible. This strategy can be applied to on-line TSA. Given a set of credible contingencies, the strategy would break the task of on-line TSA into two assessment stages [21, 31]:

Stage 1. Perform the task of dynamic contingency screening to quickly screen out contingencies that are definitely stable from a set of credible contingencies.

Stage 2. Perform a detailed assessment of dynamic performance for each contingency remaining in Stage 1.

Dynamic contingency screening is a fundamental function of an on-line TSA system. The overall computational speed of an on-line TSA system depends greatly on the effectiveness of the dynamic contingency screening, the objective of which is to identify contingencies that are definitely stable and thereby avoid further stability analysis

for these contingencies. It is from the definite classification of stable contingencies that considerable speed-up can be achieved for transient stability assessment. Contingencies that are either undecided, identified as critical, or unstable are then sent to the time-domain transient stability simulation program for additional stability analysis.

It is, hence, imperative that a dynamic contingency screening program satisfies the following five requirements [31]:

1. Reliability measure: Absolute capture of unstable contingencies as fast as possible; i.e., no unstable (single-swing or multi-swing) contingencies are missed. In other words, the ratio of the number of captured unstable contingencies to the number of actual unstable contingencies is 1.
2. Efficiency measure: High yield of screening out stable contingencies as fast as possible; i.e., the ratio of the number of stable contingencies detected to the number of actual stable contingencies is as close to 1 as possible.
3. On-line computation: Little need of off-line computations and/or adjustments in order to meet with the constantly changing and uncertain operating conditions.
4. Speed measure: High speed, i.e., fast classification for each contingency case.
5. Performance measure: Robust performance with respect to changes in power system operating conditions.

The requirement of absolute capture of unstable contingencies is a reliability measure for dynamic contingency screening. This requirement is extremely important for on-line TSA. However, it is from the nonlinear nature of the dynamic contingency screening problem that this requirement can best be met by a reliable method such as one with a strong analytical basis. The third requirement asserts that a desired dynamic contingency classifier is one that relies or little or no off-line information, computations, and/or adjustments. This requirement arises because, under current and near future power system operating environments, the correlation between on-line operational data and presumed off-line analysis data can be minimal, or in extreme cases, the two can be irrelevant to one another. In other words, in a not-too-extreme case, off-line presumed analysis data may become unrelated to on-line operational data. This uncorrelated relationship is partly attributed to the imminent bulk power transactions resulting from deregulation. The first four requirements should not be degraded by different operating conditions as dictated by the requirement for robust performance.

Several methods developed for on-line dynamic contingency screening have been reported in the literature; see, for example, [21, 31–33]. These methods can be categorized as follows: the energy function approach, the time-domain approach, and the artificial intelligence (AI) approach. The time-domain approach involves the step-by-step simulation of each contingency for a few seconds, say 2 or 3 seconds, to filter out the very stable or very unstable contingencies. This approach may suffer from an accuracy problem in identifying multi-swing stable or unstable contingencies. The AI approaches, such as the pattern recognition technique, the expert system technique, the decision tree technique, and the artificial neural network approach, all first perform extensive off-line numerical simulations aiming to capture the essential stability features of the system's dynamic behavior. They then construct a classifier attempting to correctly classify new, unseen on-line contingencies. As such, the AI approach is likely to become ineffective for on-line application to current or near-future power systems if little correlation exists between on-line operational data and presumed off-line analysis data. In addition, the existing AI-based methods unfortunately fail to meet the on-line computation requirement and cannot guarantee the reliability requirement. In this regard, the BCU classifiers can meet the requirements [21, 31].

## DIRECT METHODS FOR TRANSIENT STABILITY

The direct method evolved in the last several decades. The current direct method, the controlling unstable equilibrium point (UEP) method, uses an algorithmic procedure to determine, based on the energy function theory and controlling UEP, whether the system will remain stable, without integrating the post-fault system [16, 17, 18]. The direct method assesses the stability property of the post-fault trajectory, whose initial state is the system state when the fault is cleared, by comparing the system energy at the initial state of post-fault trajectory with a critical energy value. The direct method not only avoids the time-consuming numerical integration of the post-fault system but also provides a quantitative measure of the degree of system stability. The direct method has a solid theoretical foundation [16, 17].

Given a power system transient stability model with specified fault-on systems and a specified post-fault system, direct methods for transient stability analysis consist of four key steps:

Step 1. Construct an energy function for the post-fault power system.

Step 2. Compute the energy immediately after the fault clearing point is reached.

Step 3. Compute the critical energy for the fault-on trajectory.

Step 4. Perform transient stability assessments by comparing the energy computed at Step 2 with the critical energy computed at Step 3. If the former is smaller than the latter, then the post-fault trajectory will be stable. Otherwise, it may be unstable.

In Step 4, direct methods determine whether a post-fault power system will remain stable when the fault is cleared solely by comparing the system energy (constructed in Step 1) immediately after the fault clearing point is reached (computed in Step 2) with to a critical energy (computed in Step 3). It is hence very important to correctly calculate critical energy values.

The theoretical basis of direct methods for the direct stability assessment of a post-fault power system is the knowledge of a stability region; if the initial condition of the post-fault system lies inside the stability region of a

desired post-fault stable equilibrium point, then one can ensure without performing numerical integrations that the ensuing post-fault trajectory will converge to the desired point. Therefore, the knowledge of the stability region plays an important role in the theoretical foundation for direct methods. A comprehensive theory of stability region can be found in [30]. An overview of the energy function theory for general nonlinear autonomous dynamical systems will be presented. The energy function theory has been applied to power system transient stability models to develop a theoretical foundation for direct methods. We will also give an overview of this development.

Several methods are proposed in the literature for determining the critical energy values. The classic method, the closest UEP method proposed in the early 1970s, has been found to yield unduly conservative results when applied to power system transient stability analysis. The potential energy boundary surface (PEBS) method [34] gives fairly fast but inaccurate results (mostly overestimates). A desirable method for determining the critical energy value would be the one that can provide the most accurate approximation of the part of the stability boundary toward which the fault-on trajectory is heading, even though it might provide a very poor estimate of the other part of the stability boundary. To this end, the controlling UEP method, which uses the (connected) constant energy surface passing through the controlling UEP to approximate the relevant part of stability boundary, is the most promising method. The concept of controlling UEP and its theoretical basis will be presented in next section.

### Energy Function Theory

We consider a general nonlinear autonomous dynamical system described by the following equation:

$$\dot{x}(t) = f(x(t)) \tag{7}$$

to be the power system model under study, where the state vector $x(t)$ belongs to the Euclidean space $R^n$, and the function $f : R^n \to R^n$ satisfies the sufficient condition for the existence and uniqueness of solutions. A state vector $\hat{x}$ is called an equilibrium point of system (7) if ( $f(\hat{x}) = 0$). We say that an equilibrium point of (7) is *hyperbolic* if the Jacobian of $f(\cdot)$ at $\hat{x}$, denoted $J_f(\hat{x})$, has no eigenvalues with a zero real part. For a hyperbolic equilibrium point, it is an *(asymptotically) stable equilibrium point* if all eigenvalues of its corresponding Jacobian have negative real parts; otherwise it is an *unstable equilibrium point*. If the Jacobian of the equilibrium point $\hat{x}$ has exactly one eigenvalue with a positive real part, we call it a *type-one equilibrium point*. Likewise, $\hat{x}$ is called a *type-k equilibrium point* if its corresponding Jacobian has exactly $k$ eigenvalues with positive real parts.

Let $\hat{x}$ be a hyperbolic equilibrium point. Its stable and unstable manifolds, $W^s(\hat{x})$ and $W^u(\hat{x})$, are defined as follows:

$$\begin{aligned} W^s(\hat{x}) &:= \{x \in R^n : \Phi_t(x) \to \hat{x} \quad as \quad t \to \infty\} \\ W^u(\hat{x}) &:= \{x \in R^n : \Phi_t(x) \to \hat{x} \quad as \quad t \to -\infty\} \end{aligned} \tag{8}$$

Every trajectory in the stable manifold $W^S(\hat{x})$ converges to $\hat{x}$ as time goes to positive infinity, whereas every trajectory in the stable manifold $W^u(\hat{x})$ converges to $\hat{x}$ as time goes to negative infinity. For a stable equilibrium point, it can be shown that a number $\delta > 0$ exists such that $\|x_0 - \hat{x}\| < \delta$ implies $\Phi_t(x_0) \to \hat{x}$ as. If $(t \to \infty)$ is arbitrarily large, then $\hat{x}$ is called a *global stable equilibrium point*. Many physical systems contain multiple stable equilibrium points. A useful concept for these kinds of systems is that of the *stability region* (also called the *region of attraction*). The stability region of a stable equilibrium point $x_s$ is defined as

$$A(x_s) := \{x \in R^n : lim_{t \to \infty} \Phi_t(x) = x_s\} \tag{9}$$

From a topological point of view, the stability region $A(x_s)$ is an open, invariant, and connected set. The boundary of stability region $A(x_s)$ is called the *stability boundary* of $x_s$ and will be denoted by $\partial A(x_s)$.

We say a function $V : R^n \to R$ is an *energy function* for the system (7) if the following three conditions are satisfied:

1. The derivative of the energy function $V(x)$ along any system trajectory $x(t)$ is nonpositive, i.e.,
$$\dot{V}(x(t)) \leq 0 \tag{10}$$
2. If $x(t)$ is a nontrivial trajectory, i.e., $x(t)$, is not an equilibrium point, then, along the nontrivial trajectory $x(t)$, the set
$$\{t \in R : \dot{V}(x(t)) = 0\} \tag{11}$$
has measure zero in $R$.
3. That a trajectory $x(t)$ has a bounded value of $V(x(t))$ for $t \in R^+$ implies that the trajectory $x(t)$ is also bounded. Stating this in brief:

   That $V(x(t))$ is bounded implies $x(t)$ is also bounded.

Property (1) states that the energy function is nonincreasing along its trajectory, but it does not imply that the energy function is strictly decreasing along its trajectory. A time interval $[t_1, t_2]$ may exist such that $\dot{V}(x(t)) = 0$ for $t \in [t_1, t_2]$. Properties (1) and (2) imply that the energy function is strictly decreasing along any system trajectory. Property (3) states that the energy function is a proper map along any system trajectory but need not be a proper map for the entire state space. Recall that a proper map is a function $f : X \to Y$ such that for each compact set $(D \in Y)$, the set $f^{-1}(D)$ is compact in $X$. Property (3), which can be viewed as a "dynamic" proper map, is useful in the characterization of stability boundary. From the above definition of energy function, it is obvious that an energy function may not be a Lyapunov function.

In general, the dynamic behaviors of trajectories of general nonlinear systems could be very complicated; the asymptotic behaviors of trajectories can be quasi-periodic trajectories or even chaotic trajectories [35, 41]. If the underlying dynamical system has some special properties, then the system may admit only simple trajectories. For instance, every trajectory of system (7) having an energy function has only two modes of behaviors: Its trajectory either converges to an equilibrium point or goes to infinity (becomes unbounded) as time increases or decreases and

the stability region of the system can be completely characterized. These results are shown in the following theorems:

**Theorem 1: [16, 17] (Global behavior of trajectories).** If a function exists satisfying condition (1) and condition (2) of the energy function for general nonlinear system (7), then every bounded trajectory of system (7) converges to one of the equilibrium points.

**Theorem 2: [16, 17] (Energy function and stability boundary).** If an energy function exists for the system (7), which has an asymptotically stable equilibrium point $x_s$ (but not globally asymptotically stable), then the stability boundary $\partial A(x_s)$ is contained in the set, which is the union of the stable manifolds of the UEPs on the stability boundary $\partial A(x_s)$; i.e.,

$$\partial A(x_s) \subseteqq \bigcup_{x_i \in \{E \cap \partial A(x_s)\}} W^s(x_i)$$

Theorem 2 offers a means for completely characterizing the stability boundary of the class of nonlinear dynamical systems having energy functions: The stability boundary $\partial A(x_s)$ is contained in the union of the stable manifolds of the UEPs on the stability boundary. These stable manifolds govern the dynamical behaviors on the stability boundary. This theorem leads to the development of a theoretical foundation for direct methods.

The energy function theory presented above is applicable to transient stability models described by ordinary differential equations (ODEs). Extensions of these results to network-preserving transient stability models that are mathematically described by a set of differential and algebraic equations (DAE) can be found in Ref. 36.

## CONSTRUCTING ENERGY FUNCTIONS

It can be shown that an analytical expression of energy functions does not exist for general lossy network-preserving transient stability models [35]. Consequently, numerical energy functions must be used. We present procedures to derive numerical energy functions for structure-preserving transient stability models. Most existing network-preserving models can be rewritten as a set of general differential-algebraic equations of the following compact form [15]:

$$\begin{aligned}
0 &= -\frac{\partial U}{\partial u}(u, w, x, y) + g_1(u, w, x, y) \\
0 &= -\frac{\partial U}{\partial w}(u, w, x, y) + g_2(u, w, x, y) \\
T\dot{x} &= -\frac{\partial U}{\partial x}(u, w, x, y) + g_3(u, w, x, y) \\
\dot{y} &= z \\
M\dot{z} &= -Dz - \frac{\partial U}{\partial y}(u, w, x, y) + g_4(u, w, x, y)
\end{aligned} \tag{12}$$

where $u \in IR^l$ and $w \in IR^l$ are instantaneous variables while $x \in IR^n$, $y \in IR^n$, and $z \in IR^n$ are state variables. $T$ is a positive definite matrix, and $M$ and $D$ are diagonal positive definite matrices. Here differential equations describe generator and/or load dynamics, whereas algebraic equations express the power flow equations at each bus. $g_1(u, w, x, y)$, $g_2(u, w, x, y)$, $g_3(u, w, x, y)$, and $g_4(u, w, x, y)$ are vectors representing the effects of the transfer conductance in the network Y-bus matrix. With the aid of the singularly perturbed systems, the compact representation of the network-preserving model becomes

$$\begin{aligned}
\varepsilon_1\dot{u} &= -\frac{\partial U}{\partial u}(u, w, x, y) + g_1(u, w, x, y) \\
\varepsilon_2\dot{u} &= -\frac{\partial U}{\partial w}(u, w, x, y) + g_2(u, w, x, y) \\
T\dot{x} &= -\frac{\partial U}{\partial x}(u, w, x, y) + g_3(u, w, x, y) \\
M\dot{z} &= -Dz - \frac{\partial U}{\partial y}(u, w, x, y) + g_4(u, w, x, y)
\end{aligned} \tag{13}$$

where $\varepsilon_1$ and $\varepsilon_2$ are sufficiently small positive numbers. For the compact representation of the singularly perturbed network-preserving power system model (14) without the transfer conductance, we consider the following function $W : R^{k+l+2n+m} \to R$:

$$\begin{aligned}
W(u, w, x, y, z) &= K(z) + U(u, w, x, y) \\
&= \frac{1}{2}z^T Mz + U(u, w, x, y)
\end{aligned} \tag{14}$$

Suppose that along every nontrivial trajectory of system (13) with a bounded value of $W(u, w, x, y, z)$, the vector $(u(t), w(t), x(t))$ is also bounded for $t \in R^+$. Then $W(u, w, x, y, z)$ is an energy function for system (13).

A numerical network-preserving energy function $W_{\text{num}}(u, w, x, y)$ can be constructed by combining an analytic energy function $W_{\text{ana}}(u, w, x, y, z) = K(z) + U(u, w, x, y)$ and a path dependent potential energy $U_{\text{path}}(u, w, x, y)$; i.e.,

$$\begin{aligned}
&W_{\text{num}}(u, w, x, y, z) = W_{\text{ana}}(u, w, x, y, z) + U_{\text{path}}(u, w, x, y) \\
&= K(z) + U(u, w, x, y) + U_{\text{path}}(u, w, x, y) \\
&= K(z) + U_{\text{num}}(u, w, x, y)
\end{aligned}$$

A general methodology for the derivation of an energy function for general power system stability models can be found in Refs. 37–39 and references therein.

## ENERGY FUNCTIONS AND STABILITY REGION

We next present how to estimate the stability region of a high-dimension nonlinear system, such as a power system, via an energy function. These analytical results will be used to provide a theoretical foundation for direct methods in general and for the controlling UEP method.

We consider the following set:

$$S_v(k) = \{x \in R^n : V(x) < k\} \tag{15}$$

where $V(\cdot) : R^n \to R$ is an energy function. We shall call the boundary of set (15), $\partial S(k) := \{x \in R^n : V(x) = k\}$, the *level set* (or *constant energy surface*) and $k$ the *level value*. If $k$ is a regular value (i.e., $\nabla V(x) \neq 0$, for all $x \in V^{-1}(k)$), then by the Inverse Function Theorem, $\partial S(k)$ is a $C^r$ (n-1)-dimensional submanifold of $R^n$. Generally speaking, this set $S(k)$ can be very complicated with several disjoint connected components even for the two-dimensional case. Let

$$S(k) = S^1(k) \cup S^2(k) \cup \ldots \cup S^m(k) \tag{16}$$

where $S^i(k) \cap S^j(k) = \phi$ when $i \neq j$. That is, each of these components is connected and disjoint from each other.

Since $V(\cdot)$ is continuous, $S(k)$ is an open set. Because $S(k)$ is an open set, the level set $\partial S(k)$ is of (n-1) dimensions. Furthermore, each component of $S(k)$ is an invariant set.

Despite the possibility that a constant energy surface may contain several disjoint connected components, there is an interesting relationship between the constant energy surface and the stability boundary. This relationship is that at most one connected component of the constant energy surface $\partial S(r)$ has a nonempty intersection with the stability region $A(x_s)$. This relationship is established in Theorem 5 below.

***Theorem 5: [16, 17] (Constant energy surface and stability region).*** Let $x_s$ be a stable equilibrium point of system (7) and $A(x_s)$ be its stability region. Then, the set $S(r)$ contains only one connected component, which has a nonempty intersection with the stability region $A(x_s)$ if and only if $r > V(x_s)$

Motivated by Theorem 5, we shall use the notation $S_{x_s}(r)$ to denote the connected set of $S(r)$ (whose level value is $r$) containing the stable equilibrium point $x_s$. We drop the subscript $x_s$ of $S_{x_s}(r)$ when it is clear from the context. There is a close relation between the constant energy surfaces at different level values and the stability region $A(x_s)$. It can be shown that the connected set $S_{x_s}(r)$ with a level value $r$ smaller than the critical value is very conservative in the approximation of the stability boundary $\partial A(x_s)$. As the set $S_{x_s}(r)$ is expanded by increasing the level value $r$, the approximation gets improved until this constant energy surface hits the stability boundary $\partial A(x_s)$ at some point. This point will be shown to be an unstable equilibrium point. We call this point the *closest UEP* of the SEP $x_s$ with respect to the energy function $V(\cdot)$. Furthermore, as we increase the level value $r$, the connected set $S_{x_s}(r)$ would contain points that lie outside the stability region $A(x_s)$.

It is inappropriate to approximate the stability region $A(x_s)$ by the connected set $S_{x_s}(r)$ with a level value higher than that of the lowest point on the stability boundary $\partial A(x_s)$. Among the several disjoint connected sets of the constant energy surface, the connected set $S_{x_s}(r)$ is the best candidate to approximate the stability region $A(x_s)$ as shown in the following theorem.

***Theorem 6: [16, 17] (Topological characterization).*** Consider the nonlinear system (7) that has an energy function. Let $x_s$ be an asymptotically stable equilibrium point whose stability region $A(x_s)$ is not dense in $R^n$. Then, the point with the minimum value of the energy function over the stability boundary $\partial A(x_s)$ exists, and it must be an unstable equilibrium point.

We recall that the fundamental problem of power system transient stability analysis is concerned with whether, given a pre-fault SEP and a fault-on trajectory, the post-fault initial state is located inside the stability region of an asymptotically stable equilibrium point at which all the engineering and operational constraints are satisfied. In the context of power system transient stability analysis, we remark that, given a point in the state space (say, the initial point of the post-fault system), it is generally difficult to determine which connected component of a level set contains the point by simply comparing the energy at the given point and the energy of the level set, because a level set usually contains several disjoint connected components and these components are not easy to differentiate based on an energy function value.

Fortunately, in the context of direct methods, this difficulty can be circumvented because direct methods compute the relevant pieces of information regarding (1) a pre-fault stable equilibrium point, (2) a fault-on trajectory, and (3) a post-fault stable equilibrium point. These pieces of information are sufficient to identify the connected component of a level set that contains the initial point of a post-fault system. We next discuss the most viable direct method: the controlling UEP method.

## CONTROLLING UEP METHOD

Several methods are proposed in the literature attempting to determine accurate critical energy values; see for example, Refs. 34, 40–44. The classic method, the closest UEP method proposed in the early 1970s, when applied to power system transient stability analysis has been found to yield unduly conservative results. The origin of this conservativeness can be explained from a nonlinear system viewpoint. The closest UEP method attempts to provide an approximation for the entire stability boundary of the post-fault system, rather than for the relevant part of the stability boundary toward which the fault-on trajectory is heading. This approximation by the closest UEP method is independent of the fault-on trajectory. Thus, the closest UEP method usually gives very conservative results for transient stability analysis. The potential energy boundary surface (PEBS) method proposed by Kakimoto et al. gives fairly fast and accurate stability assessments but may give inaccurate results (both overestimates and underestimates).

A desirable method (for determining the critical energy value) would be the one that can provide the most accurate approximation of the part of a the stability boundary toward which the fault-on trajectory is heading, even though it might provide a very poor estimate of the other part of stability boundary. This is the spirit of the controlling UEP method, which uses the (connected) constant energy surface passing through the controlling UEP to approximate the part of stability boundary toward which the fault-on trajectory is heading. If, when the fault is cleared, the system state lies inside the (connected) energy surface passing through the controlling UEP, then the post-fault system must be stable (i.e., the post-fault trajectory will settle down to a stable operating point); otherwise, the post-fault system may be unstable. This is the essence of the controlling UEP method. A consensus seems to have emerged that, among several methods (for determining the critical energy value), the controlling UEP method is the most viable for direct stability analysis of practical power systems [20,45,16]. The success of the controlling UEP method, however, hinges on its ability to find the correct controlling UEP.

Given a power system model with a prefault SEP $X_s^{\text{pre}}$, a fault-on trajectory $X_f(t)$, and a post-fault (transient) sta-

bility system $S^{\text{post}}$ with a post-fault SEP $X_s^{\text{post}}$, suppose an energy function exists for the post-fault system $S^{\text{post}}$ and $X_s^{\text{pre}}$ lies inside the stability region of $X_s^{\text{post}}$. We next discuss a rigorous definition of the controlling UEP

***Definition [16].*** The controlling UEP with respect to the fault-on trajectory $X_f(t)$ is the UEP of the post-fault system $S^{\text{post}}$ whose stable manifold contains the exit point of $X_f(t)$; i.e., the controlling UEP is the first UEP whose stable manifold is hit by the fault-on trajectory $X_f(t)$ at the exit point.

This definition is motivated by the fact that a sustained fault-on trajectory must exit the stability boundary of a post-fault system and that the exit point, i.e., the point from which a given fault-on trajectory exits the stability boundary of a post-fault system, of the fault-on trajectory must lie on the stable manifold of a UEP on the stability boundary of the post-fault system. This UEP is the controlling UEP of the fault-on trajectory. Note that the existence and uniqueness of the controlling UEP with respect to a fault-on trajectory are assured by Theorem 2 and that the controlling UEP is independent of the energy function used in the direct stability assessment. With the formal definition of the controlling UEP, we are in a position to formalize the controlling UEP method.

### The Controlling UEP Method

The controlling UEP method for direct stability analysis of large-scale power systems proceeds as follows:

1. Determination of the critical energy
   - Step 1.1: Find the controlling UEP, $X_{\text{co}}$, for a given fault-on trajectory $X_f(t)$.
   - Step 1.2: The critical energy, $v_{\text{cr}}$, is the value of energy function $V(\cdot)$ at the controlling UEP; i.e., $v_{\text{cr}} = V(X_{\text{co}})$.
2. Approximation of the relevant part of stability boundary
   - Step 2.1: Use the connected constant energy surface of $V(\cdot)$ passing through the controlling UEP $X_{\text{co}}$ and containing the SEP $X_s$ to approximate the relevant part of stability boundary for the fault-on trajectory $X_f(t)$.
3. Determination of stability: Check whether the fault-on trajectory at the fault clearing time $(t_{cl})$ is located inside the stability boundary characterized in Step 2.1. This is done as follows:
   - Step 3.1: Calculate the value of the energy function $V(\cdot)$ at the time of fault clearance $(t_{cl})$ using the fault-on trajectory; i.e., $v_f = V(X_f(t_{cl}))$.
   - Step 3.2: If $v_f < v_{\text{cr}}$, then the point $X_{f(cl)}$ is located inside the stability boundary and the post-fault system is stable. Otherwise, it is unstable.

The controlling UEP method yields an approximation of the relevant part of the stability boundary of the post-fault system to which the fault-on trajectory is heading. It uses the (connected) constant energy surface passing through the controlling UEP to approximate the relevant part of stability boundary.

### Analysis of the Controlling UEP Method

The controlling UEP method asserts that the energy value at the controlling UEP be used as the critical energy for the fault-on trajectory $X_f(t)$ to assess stability. Using the energy value at another UEP as the critical energy can give erroneous stability assessment. Theorem 7 gives a rigorous theoretical justification of the controlling UEP method for direct stability analysis of post-fault systems by just comparing the energy value of the state vector at which the fault is cleared with the energy value at the controlling UEP.

***Theorem 7: (Fundamental theorem for the controlling UEP method).*** Consider a general nonlinear autonomous system that has an energy function $V(\cdot): R^n \to R$. Let $X_{\text{co}}$ be an equilibrium point on the stability boundary $\partial A(X_s)$ of this system. Let $r > V(X_s)$ and $S(r) \triangleq$ the connected component of the set $\{X \in R^n : V(X) < r\}$ containing $X_s$, and $\partial S(r)$: $\triangleq$ the (topological) boundary of $S(r)$.

Then,

1. The connected constant energy surface $\partial S(V(X_{\text{co}}))$ intersects with the stable manifold $W^s(X_{\text{co}})$ only at point $X_{\text{co}}$; moreover, the set $\partial S(V(X_{\text{co}}))$ has an empty intersection with the stable manifold $W^s(X_{\text{co}})$. In other words, $\partial S(V(X_{\text{co}})) \cap W^s(X_{\text{co}}) = X_{\text{co}}$ and $S(V(X_{\text{co}})) \cap W^s(X_{\text{co}}) = \phi$.
2. $S(V(X^u)) \cap W^s(X_{\text{co}}) = \phi$ if $X^u$ is a u.e.p. and $V(X^u) > V(X_{\text{co}})$.
3. $S(V(X^u)) \cap W^s(X_{\text{co}}) = \phi$ if $X^u$ is a u.e.p. and $V(X^u) > V(X_{\text{co}})$.
4. If $\hat{X}\hat{X}$ is not the closest UEP, then $\partial S(V(\hat{X})) \cap (\bar{A}(X_s))^c \neq \phi$.
5. Any connected path starting from a point $P \in \{S(V(X_{\text{co}})) \cap A(X_s)\}$ and passing through $W^s(X_{\text{co}})$ must hit $\partial S(V(X_{\text{co}}))$ before the path hits $W^s(X_{\text{co}})$.

We next elaborate on the above fundamental theorem. Results [1] and [5] of Theorem 7 assert that, for any fault-on trajectory $X_f(t)$ starting from a point $X_s^{\text{pre}} \in A(X_s)$ and $V(X_s^{\text{pre}}) < V(\hat{X})$, if the exit point of this fault-on trajectory $X_f(t)$ lies on the stable manifold of $X_{\text{co}}$, then this fault-on trajectory $X_f(t)$ must pass through the connected constant energy surface $\partial S(V(X_{\text{co}}))$ before it passes through the stable manifold of $X_{\text{co}}$ [thus exiting the stability boundary $\partial A(X_s)$]. Therefore, the connected constant energy surface $\partial S(V(\hat{X}_{\text{co}}))$ can be used to approximate the relevant part of the stability boundary.

Theorem 7 also shows the slightly conservative nature of the controlling UEP method in direct stability assessment. More importantly, this method can directly detect both first-swing and multiswing stability or instability, although historically direct methods have been said to be only applicable to first-swing stability analysis. Note that once the initial point of the post-fault system lies inside the stability region $A(x_s)$, the post-fault trajectory will converge to $X_s$ after one or multiple swings.

On the other hand, results [2] and [4] of Theorem 7 assert that the following two situations may occur:

Case (1): The set $S(V(X^u))$ contains only part of the stable manifold. $W^s(X_{co})$

Case (2): The set $S(V(X^u))$ contains the whole stable manifold. $W^s(X_{co})$

In case (1), the fault-on trajectory $X_f(t)$ may pass through the connected constant energy surface $\partial S(V(X^u))$ before it passes through the stable manifold $W^s(X_{co})$. In this situation, incorrect use of $X^u$ as the controlling UEP still gives an accurate stability assessment. Alternatively, the fault-on trajectory $X_f(t)$ may pass through the connected constant energy surface $\partial S(V(X^u))$ after it passes through the stable manifold $W^s(X_{co})$. In this situation, the controlling UEP method using $X^u$ as the controlling UEP, which in fact not the controlling UEP gives an inaccurate stability assessment. This classification is incorrect. In case (2), the fault-on trajectory $X_f(t)$ always passes through the connected constant energy surface $\partial S(V(X^u))$ after it passes through the stable manifold $W^s(X_{co})$. Under this situation, incorrect use of $X^u$ as the controlling UEP can give inaccurate stability assessments. In particular, it can classify the post-fault trajectory to be stable when in fact it is unstable.

Results [3] and [4] of Theorem 7 assert that the set $S(V(X^u))$ has an empty intersection with the stable manifold $W^s(X_{co})$. Under this situation, the fault-on trajectory $X_f(t)$ always passes through the connected constant energy surface $\partial S(V(X^u))$ first before it passes through the connected constant energy surface $\partial S(V(X_{co}))$. Thus, using $V(X^u)$ as the critical energy value always gives more conservative stability assessments than using that of the (exact) controlling UEP, $X_{co}$. From these cases, it is clear that for a given fault-on trajectory $X_f(t)$, if the exit point of this fault-on trajectory $X_f(t)$ lies on the stable manifold of $X_{co}$, then using the energy value at a UEP other than $X_{co}$ can give stability assessments in both directions: too conservative stability assessments (classify many stable trajectories to be unstable) or too optimistic stability assessments (classify unstable trajectories to be stable).

**Challenges in Computing Controlling UEP.** The task of finding the (exact) controlling UEP of a given fault for general power system models is very difficult. This difficulty comes in part from the following complexities:

1. The controlling UEP is a particular UEP embedded in a large-degree state-space.
2. The controlling UEP is the first UEP whose stable manifold is hit by the fault-on trajectory (at the exit point).
3. The task of computing the exit point is very involved; it usually requires a time-domain approach. I
4. The task of computing the controlling UEP is complicated further by the size and the shape of its convergence region.

It is known that, with respect to a selected numerical method, each equilibrium point has its own convergence region, i.e., the region from which the sequence generated by the numerical method starting from a point in the region will converge to the equilibrium point. It has been observed

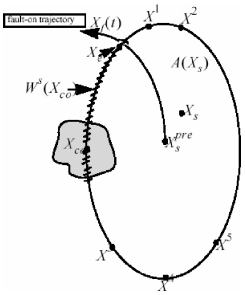


**Figure 4.** Because of "small" size and the irregular shape (fractal-like) of the convergence region of UEP with respect to Newton method, the task of computing the controlling UEP is very challenging (see the shaded area). If an initial guess is not sufficiently close to the controlling UEP, then the resulting sequence generated by, the Newton method, will diverge or converge to another exit point. This figure depicts that the sequence generated by the Newton method from the exit $X_e$ point will not converge to the controlling UEP

and theoretically investigated by several researchers that, under the Newton method, the size of the convergence region of UEP can be much smaller than that of the SEP. In addition, the convergence region of either a SEP or a UEP is a *fractal*, which refers to structures that cannot be described by the typical geometrical objects such as lines, surfaces, and solids. Irregular shape (no smooth boundaries) and self-similarity (each tiny piece we observe is similar to the form of the entire shape) are characteristics of fractals (Fig. 4.) Unfortunately, finding an initial guess sufficiently close to the controlling UEP is a difficult task.

The complexity (3) also calls into doubt the correctness of any attempt to directly compute the controlling UEP of a power system stability model. The only one method that can directly compute the controlling UEP of a power system stability model is the time-domain approach. This complexity can serve to explain why many methods proposed in the literature fail to compute the controlling UEP. It is because these methods attempt to directly compute the controlling UEP of the power system stability model that is, as pointed out in complexity (3), difficult if not impossible to compute without using the time-domain approach.

The ability to compute the controlling UEP is vital in direct stability analysis. It may prove fruitful to develop a tailored solution algorithm for finding controlling UEPs by exploiting special properties as well as some physical and mathematical insights of the underlying power system model. We will discuss in great detail such a systematic method, called the BCU method, along this line for finding controlling UEPs for power system models.

## BCU METHOD

We next discuss a method that does not attempt to directly compute the controlling UEP of a power system stability model (original model); instead it computes the controlling UEP of a reduced-state model, and then it relates the controlling UEP of the reduced-state model to the controlling UEP of the original model.

A systematic method, called the boundary of stability region based controlling unstable equilibrium point method (BCU method), to find the controlling UEP was developed [46, 47]. The method was also given other names such as the exit point method [6,48,49] and the hybrid method [50]. The BCU method has been evaluated in a large-scale power system, and it has been compared favorably with other methods in terms of its reliability and the required computational efforts [48, 49]. The BCU method has been studied by several researchers; see for example [51–56]. Descriptions of the BCU method can be found in books such as Refs. 3,4,6 and 50. The theoretical foundation of BCU method has been established in. The Refs. 15, 46, and 57 BCU method and BCU classifiers have several practical applications. For example, a demonstration of the capability of the BCU method for on-line transient stability assessments using real-time data was held at two utilities, the Ontario Hydro Company and the Northern States Power Company [58, 59]. The BCU method was implemented as an EPRI TSA software package that was integrated into an EMS installed at the control center for the Northern States Power Company [19]. A TSA system, composed of the BCU classifiers, the BCU method, and a time-domain simulation engine, was developed and integrated into the Ranger EMS system [60]. The TSA system has been installed and commissioned, as part of an EMS system at several energy control centers. The BCU method has been applied to fast derivation of power transfer limits [61] and applied to real power rescheduling to increase dynamic security [62]. The BCU method has been improved, expanded, and extended into the integrated package of TEPCO-BCU [33,46,47,63–65].

We next present an overview of the BCU method from two viewpoints: numerical aspects and theoretical aspects. In developing a BCU method for a given power system stability model, the associated artificial, reduced-state model must be defined. To explain the reduced-state model, we consider the following generic network-preserving transient stability model:

$$\begin{aligned} 0 &= -\frac{\partial U}{\partial u}(u, w, x, y) + g_1(u, w, x, y) \\ 0 &= -\frac{\partial U}{\partial w}(u, w, x, y) + g_2(u, w, x, y) \\ T\dot{x} &= -\frac{\partial U}{\partial x}(u, w, x, y) + g_3(u, w, x, y) \\ \dot{y} &= z \\ M\dot{z} &= -Dz - \frac{\partial U}{\partial y}(u, w, x, y) + g_4(u, w, x, y) \end{aligned} \tag{17}$$

where $U(u, w, x, y)$ is a scalar function. It has been shown that the above canonical representations can represent existing transient stability models. In the context of the BCU method, the above model is termed as the original model. Regarding the original model (17), we choose the following differential-algebraic system as the reduced-state model associated with the original model (17).

$$\begin{aligned} 0 &= -\frac{\partial U}{\partial u}(u, w, x, y) + g_1(u, w, x, y) \\ 0 &= -\frac{\partial U}{\partial w}(u, w, x, y) + g_2(u, w, x, y) \\ T\dot{x} &= -\frac{\partial U}{\partial x}(u, w, x, y) + g_3(u, w, x, y) \\ \dot{y} &= -\frac{\partial U}{\partial y}(u, w, x, y) + g_4(u, w, x, y) \end{aligned} \tag{18}$$

There are several close relationships between the reduced-state model (18) and the original model (17). The fundamental ideas behind the BCU method can be explained as follows. Given a power system stability model (which admits an energy function), say the original model (17), the BCU method first explores the special properties of the underlying model with the aim of defining a reduced-state model, say the model described in (18), such that the following static as well as dynamic relationships are met

**Static Properties**

(S1) The locations of equilibrium points of the reduced-state model (18) correspond to the locations of equilibrium points of the original model (17). For example, $(\hat{u}, \hat{w}, \hat{x}, \hat{y})$ is an equilibrium point of the reduced-state model if and only if $(\hat{u}, \hat{w}, \hat{x}, \hat{y}, 0)$ is an equilibrium point of the original model (17), where $0 \in R^m$ and $m$ is an appropriate positive integer.

(S2) The types of equilibrium points of the reduced-state model are the same as that of the original model. For example, $(u_s, w_s, x_s, y_s)$ is a stable equilibrium point of the reduced-state model if and only if $(u_s, w_s, x_s, y_s, 0)$ is a stable equilibrium point of the original model. $(\hat{u}, \hat{w}, \hat{x}, \hat{y})$ is a type-k equilibrium point of the reduced-state model if and only if $(\hat{u}, \hat{w}, \hat{x}, \hat{y}, 0)$ is a type-k equilibrium point of the original model.

**Dynamical Properties**

(D1) An energy function for the artificial, reduced-state model (18) exists.

(D2) An equilibrium point, say, $(\hat{u}, \hat{w}, \hat{x}, \hat{y})$ is on the stability boundary of the reduced-state model (18) if and only if the equilibrium point $(\hat{u}, \hat{w}, \hat{x}, \hat{y}, 0)$ is on the stability boundary of the original model (17).

(D3) It is computationally feasible to efficiently detect the point at which the projected fault-on trajectory $(u(t), w(t), x(t), y(t))$ hit the stability boundary $\partial A(u_s, w_s, x_s, y_s)$ of the post-fault reduced-state model (18) without resorting to an iterative time-domain procedure to compute the exit point of the post-fault reduced-state model (18).

The dynamic relationship (D3) plays an important role in the development of the BCU method to circumvent the difficulty of applying an iterative time-domain procedure to compute the exit point on the original model. The BCU method then finds the controlling UEP of the artificial, reduced-state model (18) by exploring the special structure of the stability boundary and the energy function of

the reduced-state model (18). Next, it relates the controlling UEP of the reduced-state model (18) to the controlling UEP of the original model (17).

The fundamental ideas behind the BCU method can be explained in the following. Given a power system stability model (which admits an energy function), the BCU method first explores special properties of the underlying model with the aim to define an artificial, state-reduced model such that certain static as well as dynamic relationships are met. The BCU method then finds the controlling UEP of the state-reduced model by exploring the special structure of the stability boundary and the energy function of the state-reduced model. Third, it relates the controlling UEP of the state-reduced model to the controlling UEP of the original model. In summary, given a power system stability model, a corresponding version of the BCU method exists. The BCU method does not compute the controlling UEP directly on the original model because, as pointed out, the task of computing the exit point of the original model, a key step to compute the controlling UEP, is very difficult and usually requires the time-domain approach. Instead, the BCU method (1) explores the special structure of the underlying model so as to define an artificial, state-reduced model that captures all the equilibrium points on the stability boundary of the original model; and then (2) computes the controlling UEP of the original model via computing the controlling UEP of the artificial model, which can be computed without resorting to the time-domain approach.

### A Conceptual BCU Method

Step 1. From the fault-on trajectory $[u(t), \omega(t), x(t), y(t), z(t)]$ of the network-preserving model (17), detect the exit point $(u^*, w^*, x^*, y^*)$ at which the projected trajectory $[u(t), \omega(t), x(t), y(t)]$ exits the stability boundary of the post-fault reduced-state model (18).

Step 2. Use the exit point $(u^*, w^*, x^*, y^*)$, detected in Step 1, as the initial condition and integrate the post-fault reduced-state model to an equilibrium point. Let the solution be $(u_{co}, w_{co}, x_{co}, y_{co})$.

Step 3. The controlling UEP with respect to the fault-on trajectory of the original network-preserving model (17) is $(u_{co}, w_{co}, x_{co}, y_{co}, 0)$. The energy function at $(u_{co}, w_{co}, x_{co}, y_{co}, 0)$ is the critical energy for the fault-on trajectory $[u(t), \omega(t), x(t), y(t), z(t)]$.

Steps 1 and 2 of the conceptual BCU method compute the controlling UEP of the reduced-state system. Note that starting from the exit point $(u^*, w^*, x^*, y^*)$, Step 2 of the conceptual BCU method, will converge to an equilibrium point. The controlling UEP always exists and is unique, and the stable manifold of controlling UEP of the reduced-state system $(u_{co}, w_{co}, x_{co}, y_{co})$ contains the exit point $(u^*, w^*, x^*, y^*)$ (Fig. 5.) Step 3 relates the controlling UEP of the reduced-state system (with respect to the projected fault-on trajectory) to the controlling UEP of the original system with respect to the original fault-on trajectory.

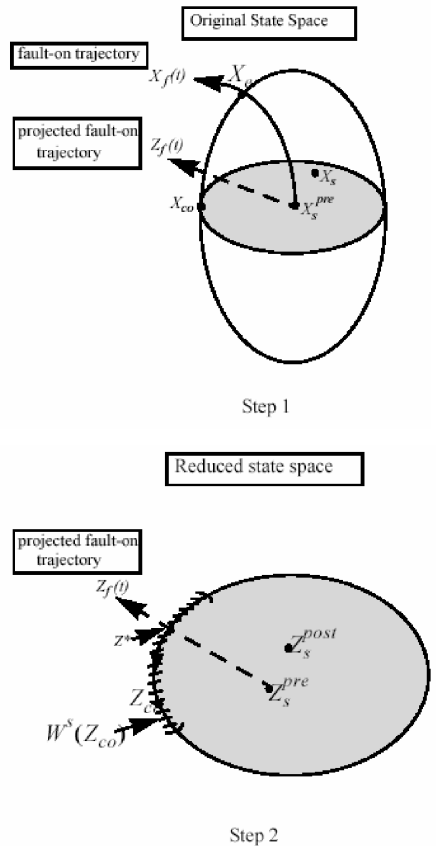


**Figure 5.** Steps 1 and 2 of the conceptual BCU method.

### Theoretical Basis

Some analytical results showing that, under certain conditions, the original model (17) and the artificial, reduced-state model (18) satisfy static relationships (S1) and (S2) as well as dynamic relationships (D1) and (D2) can be found in [46, 57]. A computational scheme has been developed and incorporated into the BCU method to satisfy dynamic relationship (D3). We next verify the static relationship.

***Theorem 8: (Static relationship).*** Let $(u_s, w_s, x_s, y_s)$ be a stable equilibrium point of the reduced-state model (18). If the following conditions are satisfied:

1. Zero is a regular value of $\dfrac{\partial^4 U(u_i, w_i, x_i, y_i)}{\partial u \partial w \partial x \partial y}$ for all the UEP $(u_i, w_i, x_i, y_i), i = 1, 2, \ldots, k$ on the stability boundary $\partial A(u_s, w_s, x_s, y_s)$.
2. The transfer conductance of reduced-state model (18) is sufficiently small. Then, $(\hat{u}, \hat{w}, \hat{x}, \hat{y})$ is a type-k equilibrium point of reduced-state model (18) if and only if $(\hat{u}, \hat{w}, \hat{x}, \hat{y}, 0)$ is a type-k equilibrium point of the original model (17).

Theorem 8 asserts that, under the stated conditions, the static properties (S1) and (S2) between original model (17) and the reduced-state model (18) hold. It can be shown that a numerical energy function exists for the reduced-state model (18). More specifically, it can be shown that for

any compact set S of the state-space of model (18), there is a positive number $\alpha$ such that, if the transfer conductance of the model satisfies $|G| < \alpha$, then there is an energy function defined on this compact set S. The examination of the dynamic property (D2) can be found in Refs. 46 and 57.

## NUMERICAL BCU METHOD

There are several possible ways to numerically implement the conceptual BCU method for network-preserving power system models. A numerical implementation of this method along with several numerical procedures necessary are presented in this section.

### A Numerical BCU Method

Step 1. Integrate the fault-on system of the original model (19) to obtain the (sustained) fault-on trajectory $[u(t), w(t), x(t), y(t), z(t)]$ until the point $(u^*, w^*, x^*, y^*)$ at which the projected trajectory $[u(t), w(t), x(t), y(t)]$ reaches its first local maximum of the numerical potential energy function $U_{\text{num}}(., ., ., .)$ along the projected trajectory.

Step 2. Apply the stability-boundary-following procedure starting from the point $(u^*, w^*, x^*, y^*)$ until the point at which the (one-dimensional) local minimum of the following norm of the post-fault, reduced-state system is reached; i.e.,

$$\begin{aligned}
&\left\| \frac{\partial U}{\partial u}(u, w, x, y) + g_1(u, w, x, y) \right\| \\
&+ \left\| \frac{\partial U}{\partial w}(u, w, x, y) + g_2(u, w, x, y) \right\| \\
&+ \left\| \frac{\partial U}{\partial x}(u, w, x, y) + g_3(u, w, x, y) \right\| \\
&+ \left\| \frac{\partial U}{\partial y}(u, w, x, y) + g_4(u, w, x, y) \right\|
\end{aligned}$$

Let the local minimum of the above norm be occurred at the point $(u_0^*, w_0^*, x_0^*, y_0^*)$.

Step 3. Use the point $(u_0^*, w_0^*, x_0^*, y_0^*)$ as the initial guess and solve the following set of nonlinear algebraic equations:

$$\begin{aligned}
&\left\| \frac{\partial U}{\partial u}(u, w, x, y) + g_1(u, w, x, y) \right\| \\
&+ \left\| \frac{\partial U}{\partial w}(u, w, x, y) + g_2(u, w, x, y) \right\| \\
&+ \left\| \frac{\partial U}{\partial x}(u, w, x, y) + g_3(u, w, x, y) \right\| \\
&+ \left\| \frac{\partial U}{\partial y}(u, w, x, y) + g_4(u, w, x, y) \right\| = 0
\end{aligned}$$

Let the solution be $(u_{\text{co}}, w_{\text{co}}, x_{\text{co}}, y_{\text{co}})$.

Step 4. The controlling UEP with respect to the fault-on trajectory $[u(t), w(t), x(t), y(t)]$ of the original system is $(u_{\text{co}}, w_{\text{co}}, x_{\text{co}}, y_{\text{co}}, 0)$.

***Remarks***

1. In Step 1, the projected trajectory $[u(t), w(t), x(t), y(t)]$ can be viewed as the projection of the original fault-on trajectory on the state-space of the reduced-state system (18). The first local maximum of the numerical potential energy function $U_{\text{num}}(., ., ., .)$ along the projected trajectory is an approximated exit point at which the projected trajectory intersects with the stability boundary of the reduced-state system (18).
2. In Step 2, a stability-boundary-following procedure, presented below, is developed to guide the search process for CUEP of the reduced-state system starting from the point $(u^*, w^*, x^*, y^*)$ by moving along the stability boundary of the reduced-state system (18) toward the CUEP. During the search process, the point $(u_0^*, w_0^*, x_0^*, y_0^*)$ has the local minimum of the norm among all computed points in the search process. The norm is a measure of distance between the current point and an equilibrium point. This point is also termed as the minimum gradient point (MGP).
3. The reduced-state system can be numerically stiff, and a stiff differential equation solver should be used to implement Step 2 of the numerical network-preserving BCU method.
4. Without the stability-boundary-following procedure implemented in Step 2, the search process can move away from CUEP, making the corresponding MGP distant from the CUEP and causing the divergence of the Newton method.
5. n Step 3, the MGP is used as an initial guess for the Newton method to compute the controlling UEP. It is well known that if the MGP is sufficiently close to the controlling UEP, then the sequence generated by the Newton method starting from the MGP will converge to the controlling UEP; otherwise, the sequence may converge to another equilibrium point or diverge (Fig. 6.). A robust nonlinear algebraic solver (with a large convergence region) is desirable in Step 3 of the numerical BCU method.
6. Note that Steps 1 to 3 of the above numerical network-preserving BCU method compute the controlling UEP of the reduced-state system (18) and Step 4 relates the controlling UEP of the reduced-state system to the controlling UEP of the original system (17).
7. From a computational viewpoint, the exit point is characterized by the first local maximum of the potential energy along the (sustained) fault-on trajectory. To find the exit point, one can compute the dot-product of the fault-on speed vector and post-fault power mismatch vector at the each integration step. When the sign of dot-product changes from positive to negative, the exit point is detected.

**Numerical Detection of Exit Point.** A numerical procedure for accurate detection of exit point in Step 1 of numerical BCU method by employing the linear interpolation method is described in the following:

Step 1. Integrate the fault-on trajectory until the dot product changes sign, say between the interval $[t_1, t_2]$.

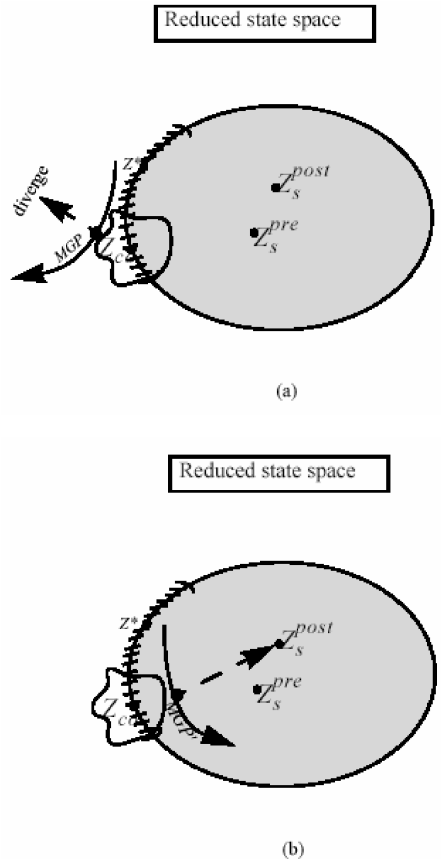


**Figure 6.** If the MGP does not lie inside the convergent region of the Newton method, then the sequence generated by the Newton method starting from the MGP will not converge to the controlling UEP. The sequence may diverge as illustrated in (a), or it may converge to the stable equilibrium point as illustrated in (b).

Step 2. Apply the linear interpolation to the interval $[t_1, t_2]$, which results in an intermediate time $t_0$ where the interpolated dot product is expected to be zero. Compute the exact dot product at $t_0$ for the post-fault reduced-state system. If the value is smaller than a threshold value, the exit point is obtained. Exit loop.

Step 3. If the dot product is positive, then replace $t_1$ with $t_0$; otherwise replace $t_2$ with $t_0$ and go to Step 2.

To find an adequate MGP for reliably computing the controlling UEP, a stability-boundary-following procedure to guide the search process for the MGP starting from the exit point and move along the stability boundary of the state-reduced system is described below:

**Stability-Boundary-Following Procedure.**

Step 1. Integrate the post-fault reduced-state system starting from the exit point for a few time-steps, say, 4 to 5 steps of integration; let the new point be termed the current point on the trajectory.

Step 2. Construct a ray connecting the current point on the trajectory and the SEP of the post-fault reduced-state system.

Step 3. Move along the ray starting from the current point and detect the point with the first local maximal potential energy, which is an energy function for the reduced-state system, along the ray. In practical implementation, this task is to check the zero crossing of the dot product between the power mismatch and the speed. The sign of the dot product at the current point determines the direction of the local maximal search. Replace the current point with the point with the first local maximal potential energy.

Step 4. Repeat Steps 1–3 until a point where the norm of the post-fault reduced-state is lower than a threshold value is reached. This point is a desired MGP.

The analytical basis for the above procedure is the structure of the stability boundary of the reduced-state system. It can be shown that the stability boundary of the original system (respectively, the reduced-state system) is composed of the stable manifold of the u.e.p on the stability boundary. The controlling UEP is the u.e.p whose stable manifold contains the exit point of the fault-on trajectory on the stability boundary of the original system. Moreover, controlling UEP is usually of type-1 (the UEP whose corresponding Jacobian matrix contains only one eigenvalue

with a positive real part). The type-1 u.e.p has the nice feature of being a "SEP" inside the stability boundary. Furthermore, the stability boundary is an "attracting" set in the state space. Hence, if one can confine the entire search process to a neighborhood close to the stability boundary of the post-fault reduced-state system, then the search process will likely obtain an MGP close to the controlling u.e.p, facilitating the convergence of Newton method. The stability-boundary-following procedure described above offers such a capability. We note that in Step 3 of the stability-boundary-following procedure, the task of updating the point along the post-fault reduced-state trajectory with the point having a local maximal energy function along the ray amounts to confine the MGP search process close to the stability boundary.

## GROUP-BASED BCU METHOD

The one-parameter transversality conditions play an important role in the theoretical foundation of the conceptual BCU method [46, 57]. Under this condition, the reduced-state system shares the same UEPs as the original system on the stability boundaries of both systems. Note that as this condition is a sufficient condition, the reduced-state system and the original system may still share the same UEPs on their stability boundaries, even though the one-parameter transversality condition is not satisfied. However, because of the complexity of practical power system models, the one-parameter transversality conditions may not be always satisfied [51–54].

We can take a different approach for verifying the one-parameter transversality condition. Instead of checking the one-parameter transversality condition and the small-transfer-conductance condition, we propose to directly check whether the UEP $(u^*_{co}, w^*_{co}, x^*_{co}, y^*_{co}, 0)$ lies on the stability boundary of the original model, i.e., check the dynamic property (D2) directly. We will also term the dynamic property (D2) the *boundary property*. It can be shown that the boundary property holds for sufficient damping systems, whereas it may not hold for low damping systems. The issue of how to determine the critical damping value above which the boundary property holds remains open. The critical damping value seems to depend on a variety of factors, including network topology, loading condition, and system models used. To overcome this issue, we propose the development of a group-based BCU method.

We have observed, through our intensive numerical simulations, that the controlling UEPs computed by the BCU method with respect to a set of contingencies tend to be close to each other. These controlling UEPs are close to each other in the state space, whereas the locations where the faults of the set of contingencies occur are close in the geographical sense. These controlling UEPs are said to form a group. These contingencies are referred to as a group of coherent contingencies.

The idea behind the development of the group-based BCU method is based on observations that the contingency list for transient stability assessment is composed of groups of coherent contingencies. Some groups may contain a large number of contingencies, whereas others may contain a small number. This idea is similar, but not related, to the ideas behind the development of dynamic network reduction methods, which are based on the observation of the formation of coherent generators after a contingency. Coherency is an observed phenomenon in power systems where certain generators tend to swing together after a disturbance.

The concept of a group of coherent contingencies will prove to be useful in several applications such as corrective control and preventive control. The coordinates of the controlling UEP in each group of coherent contingencies provide useful information on how to design controls to stabilize a power system or to enhance stability with respect to a set of contingencies.

Extensive computation experience reveals that if the controlling UEP (CUEP) of the reduced-state system lies on the stability boundary of the original system, then it is indeed the CUEP of the original system. This observation, which is very important, brings up an important numerical question, i.e., how to check whether or the CUEP of the reduced-state system lies on the stability boundary of the original system. This property is referred to as the *boundary property* of the UEP. By checking the boundary property, one can ascertain whether the UEP of the reduced-state system computed by the BCU method is the controlling UEP of the original system, without the need of checking the one-parameter transversality condition. It seems that the only numerical method capable of checking the boundary property is the one based on an iterative time-domain process.

An effective time-domain process to check the boundary property for the entire group of coherent contingencies, rather than just for on contingency, has been developed. By checking the boundary property, one can ascertain whether the UEP of the reduced-state system computed by the BCU method is the controlling UEP of the original system, without needing to check the one-parameter transversality condition. To assure the correct grouping of coherent contingencies, we have introduced the concept of *SEP separation*. This concept seens effective for identifying whether contingencies in the same group are correctly grouped. In addition, by virtue of SEP separation, contingencies within each group can be quickly regrouped. Once a group of coherent contingencies has been formed, one only needs to concentrate on the contingencies with the largest and smallest SEP separation in the same group. In this manner, a complete check of the boundary property for each contingency in each group can be avoided and a great deal of computational work can be saved.

The group-based BCU method has several advantages over any existing direct stability methods. For instance, the group-based BCU method ensures the reliability of the BCU method. In addition, the group-based BCU method can reduce the conservativeness of the BCU method. The method captures the inherent characteristics of coherent contingencies. It reduces the large number of contingencies, whose corresponding CUEP boundary property needs to be checked, to a small number. The group-based BCU method is a strict, systematic, yet reliable method to perform stability assessment for a complete list of contingencies. Compared with the conventional TSA procedure, the

increase of computational time of the group-based BCU method is mild because of the development of contingency reranking by the SEP separation in each coherent group.

## BCU CLASSIFIERS

We present a sequence of seven (improved) BCU classifiers for on-line dynamic contingency screening, developed in Refs. 31, 33, and 46. Improved BCU classifiers are designed to meet the five requirements for dynamic contingency screening. In particular, the BCU classifiers can achieve absolute capture of unstable contingencies, i.e., no unstable (single-swing or multiswing) contingencies are missed. In other words, the ratio of the captured unstable contingencies to the actual critical contingencies is 1 for both test systems. Furthermore, the yield of dropout, i.e., the ratio of dropped-out stable contingencies to actual stable contingencies), of BCU classifiers is very high. These simulation results reveal that the proposed improved BCU classifiers can be highly reliable and effective for on-line dynamic security assessments.

The analytical basis of BCU classifiers is based mainly on the three steps of the BCU method and the dynamic information derived during the computational procedure of the BCU method. A large majority of the computational efforts required in the improved BCU method are involved in computing the three important state points: the exit point (step 1), the minimum gradient point (step 2), and the controlling UEP (step 3). Useful stability information can be derived from these three points for developing effective schemes for dynamic contingency screening. We next present the design of each BCU classifier along with its analytical basis.

### Classifier I: (Classifier for SEP Problem)

This classifier is designed to screen out potentially unstable contingencies. The basis for this classifier is insufficiency in the size of the post-fault stability region or in the extreme case, the nonexistence of a post-fault stable equilibrium point. This is explained as follows. This classifier also checks whether a network island is formed after the contingency.

For direct methods to be applicable, the following three conditions need to be satisfied: (1) The post-fault equilibrium point is asymptotically stable, (2) the pre-fault stable equilibrium point $\delta_{so}$ and the post-fault equilibrium point $\delta_s$ are close to each other (so that using a nonlinear algebraic solver, such as the Newton method, with $\delta_{so}$ as the initial guess, will lead to $\delta_s$), and (3) the pre-fault stable equilibrium point $\delta_{so}$ lies inside the stability region of the post-fault equilibrium point $\delta_s$. If the pre-fault SEP lies outside the stability region of the post-fault SEP, $\delta_s$, it is very likely that the post-fault trajectory will not approach $\delta_s$, and is, hence, potentially unstable. In this classifier, two indices are designed to identify the contingencies that have the convergence problem of computing post-fault stable equilibrium points.

- $I_{\text{smax}}$: the maximum number of iterations in computing the (post-fault) stable equilibrium point.
- $\delta_{\text{smax}}$: the maximum angle difference between the pre-fault stable equilibrium point and the computed (post-fault) stable equilibrium point.

### Classifier II (Highly Stable Classifier)

This classifier is intended to screen out highly stable contingency cases. Additional stability analysis is unnecessary for highly stable contingencies. Screening out highly stable contingencies can greatly improve the goal of high yield for dynamic contingency screening. If the PEBS crossing cannot be found in the time interval $[0, T_{\text{exit}}]$, and if the potential energy difference $V_p(\delta(T_{\text{exit}}))$ is greater than zero but less than the threshold value $V_{\text{pel}}$, and if the maximum angle difference $\delta_{\text{smax}}$ is less than a threshold value, then the contingency case is highly stable and no further analysis is needed.

### Classifier III (Classifier for Exit Point Problem)

A key step in the BCU method is to integrate the (post-fault) state-reduced system starting from the exit point to find the minimum gradient point that will be used as an initial guess for computing the controlling UEP. A problem, called the *minimum gradient point problem*, may arise during the integration of the state-reduced system. The problem is described by the following: (1) there is no minimum gradient point in the simulated trajectory of the (post-fault) state-reduced system, or (2) the minimum gradient point lies in such a region that another UEP, instead of the controlling UEP, is obtained when a nonlinear algebraic solver is used to solve $\sum_{i=1}^{n} \| f_i(\delta) \| = 0$. The causes of the minimum gradient point problem can be explained from a computational viewpoint. However, the minimum gradient point problem usually damages the effectiveness and accuracy of the BCU method.

### Classifier IV (Classifier for Stability-Boundary-Following Problem)

This classifier is intended to screen out potentially unstable contingencies based on some dynamic information during the minimum gradient point search. If the stability-boundary-following fails during the minimal gradient point search, then it indicates the CUEP cannot be found by the BCU method for the study contingency and the contingency is sent to the time-domain simulation program for additional analysis.

### Classifier V (Classifier for Convergence Problem)

This classifier is designed to detect the convergence problem of computing the controlling UEP. In this classifier, the maximum number of iterations, say $I_{\text{umax}}$, in computing the controlling UEP starting from the minimum gradient point is used to detect such a problem. If the required number of iterations is more than a prespecified number, then the corresponding contingency is viewed as having a numerical divergence problem and is classified as unstable.

The convergence region of the Newton method is known to have a fractal boundary. Using the Newton method, it

has been observed that the region of the starting point that converges to a stable equilibrium point is more significant than that of a unstable equilibrium point such as the controlling UEP. Thus, in regular power flow calculation, the initial guess can be chosen near the stable equilibrium point to safely lie within the convergence region so that, after a few iterations, it converges to the desired stable equilibrium point. This explains why the fractal nature of the convergence region of Newton method has been unnoticed in power flow study for so long. As power flow study has been expanded to compute unstable equilibrium points for applications such as direct transient stability analysis and low-voltage power flow solutions for voltage collapse analysis, the fractal nature and the different size of the convergence region have become more pronounced. Unfortunately, this nature must be taken into account when a unstable equilibrium point is to be sought.

### Classifier VI (Classifier for Incorrect CUEP Problem)

The problem is described as follows: It converges to a wrong controlling UEP; i.e., the minimum gradient point lies in such a region that another UEP, instead of the controlling UEP, is obtained when a nonlinear algebraic solver is used to solve $\sum_{i=1}^{n} \| f_i(\delta) \| = 0$. In this classifier, both the coordinate of the obtained UEP and the angle difference between the MGP and the obtained UEP are used as indices to detect the problem.

### Classifier VII (Controlling UEP Classifier)

The remaining unclassified contingencies are then sent to BCU classifier VII for final classification. This classifier uses the energy value at the controlling UEP as the critical energy to classify each remaining contingency as (definitely) stable or (potentially) unstable. If the energy value at the fault clearing time is less than the energy value at the controlling UEP, then the corresponding contingency is (definitely) stable; otherwise it is (potentially) unstable. The theoretical basis of this classifier is the CUEP method. The index used in this classifier is the energy value at the fault clearing time, whereas the threshold value for this index is the energy value at the controlling UEP.

In summary, given a list of credible contingencies to the seven BCU classifiers, the first classifier is designed to screen out those contingencies with convergence problems in computing post-fault stable equilibrium points. The second and third classifiers, based on Step 1 of the BCU method, are the fastest ones. They use the energy value at the exit point on the stability boundary of the reduced-state model as an approximation for the critical energy. The second classifier is designed to drop those contingencies that are highly stable, whereas the third is designed to screen out those contingencies that may cause computational difficulties for the BCU method and, hence, may damage the reliability of the following BCU classifiers. The fourth classifier screens out those contingencies that cause failure in finding the MGP. The fifth classifier screens out the contingencies with the problem of converging to the controlling UEP. The sixth classifier drops those contingencies with the problem of incorrect CUEP. The seventh classifier uses the energy at the controlling u.e.p as the critical energy to classify every contingency left over from the previous classifiers into two classes: stable contingencies and unstable contingencies. This classifier is based on Step 3 of the BCU method.

Contingencies that are classified as definitely stable at each classifier are eliminated from additional analysis. It is because of the definite classification of stable contingencies that considerably increased speed for dynamic security assessment can be achieved. Contingencies that are either undecided or identified as unstable are then sent to the time-domain transient stability simulation program for further stability analysis. Note that the conservative nature of the BCU method guarantees that the results obtained from the seven dynamic contingency classifiers are also conservative; i.e., no unstable cases are misclassified as stable. Classifying a stable contingency, either first-swing or multiswing, as unstable is the only scenario in which the BCU classifiers give conservative classifications.

From a practical viewpoint, it is worth noting that a time-domain simulation program is needed to further analyze those contingencies that are only dropped out from Classifiers I, III, IV, V, and VI. Therefore, the efficiency of the proposed BCU classifiers depends on the ratio of those contingencies screened out from Classifiers II and VII with respect to the total stable contingencies, i.e., the yield of drop-out of stable contingencies. Note that the number of stable contingencies is not a criterion for evaluating performance because it depends on several factors, among which the loading condition, network topology, and contingency selection all play an important role. The seven BCU classifiers perform the process of dynamic contingency screening in a sequential order.

### Numerical Studies

The improved BCU classifiers has been extensively evaluated on a practical power system transient stability model. A total of 507 contingencies on the test system with heavy loading conditions and ZIP load model and a total of 466 contingencies on the test system with medium loading conditions and non-smooth load model were applied. The type of faults considered in the evaluation were three-phase faults with fault locations at both generator and load buses. Some contingencies are faults that were cleared by opening double circuits, whereas others are faults that were cleared by opening the single circuit. Two load models were employed in the simulation: the non-smooth load model and the ZIP load model with the composition of the 20% constant current, 20% constant power, and 60% constant impedance. Both severe and mild faults were considered. All faults were assumed to have been cleared after 0.07 s. A time-domain stability program was used to numerically verify all classification results. Simulation results on both systems are presented next.

A summary of dynamic contingency screening by the improved BCU classifiers and the time-domain stability program on the test system with heavy-loading condition and ZIP load model for the undamped factor and damped factor is displayed in Table 1 and Table 2, respectively. A summary

Table 1. BCU classifiers on a test system (undamped, heavy-loading): ZIP model

| Tools | Results | I (U) | II (S) | III (U) | IV (U) | V (U) | VI (U) | VII (S) | VII (U) | Total |
|---|---|---|---|---|---|---|---|---|---|---|
| BCU Classifiers | Drop-Out cases | 83 | 6 | 0 | 2 | 12 | 1 | 378 | 25 | 507 |
| Time-Domain | Stable | 6 | 6 | 0 | 2 | 12 | 1 | 378 | 17 | 422 |
| | Unstable | 77 | 1 | 0 | 0 | 0 | 0 | 0 | 8 | 85 |

Table 2. BCU classifiers on a test system (damped, heavy-loading): ZIP model

| Tools | Results | I (U) | II (S) | III (U) | IV (U) | V (U) | VI (U) | VII (S) | VII (U) | Total |
|---|---|---|---|---|---|---|---|---|---|---|
| BCU Classifiers | Drop-Out cases | 83 | 16 | 0 | 1 | 11 | 1 | 369 | 26 | 507 |
| Time-Domain | Stable | 9 | 16 | 0 | 1 | 11 | 1 | 369 | 18 | 425 |
| | Unstable | 74 | 0 | 0 | 0 | 0 | 0 | 0 | 8 | 82 |

Table 3. BCU classifiers on a test system (undamped, medium-loading): non-smooth model

| Tools | Results | I (U) | II (S) | III (U) | IV (U) | V (U) | VI (U) | VII (S) | VII (U) | Total |
|---|---|---|---|---|---|---|---|---|---|---|
| BCU Classifiers | Drop-Out cases | 26 | 8 | 0 | 4 | 4 | 0 | 419 | 5 | 466 |
| Time-Domain | Stable | 4 | 8 | 0 | 4 | 4 | 0 | 419 | 5 | 444 |
| | Unstable | 22 | 0 | 0 | 0 | 0 | 0 | 0 | 0 | 22 |

Table 4. BCU classifiers on a test system (damped, medium-loading): non-smooth model

| Tools | Results | I (U) | II (S) | III (U) | IV (U) | V (U) | VI (U) | VII (S) | VII (U) | Total |
|---|---|---|---|---|---|---|---|---|---|---|
| BCU Classifiers | Drop-Out cases | 26 | 11 | 0 | 4 | 3 | 0 | 418 | 4 | 466 |
| Time-Domain | Stable | 4 | 11 | 0 | 4 | 3 | 0 | 418 | 4 | 444 |
| | Unstable | 22 | 0 | 0 | 0 | 0 | 0 | 0 | 0 | 22 |

of dynamic contingency screening on the test system with medium-loading and non-smooth load model for undamped factor and damped factor is displayed in Table 3 and Table 4, respectively. A detailed explanation is presented below.

1. Test system with heavy-loading. For the test system with heavy-loading conditions, ZIP load model, and undamped effect, we summarized the evaluation of BCU classifiers on a total of 507 contingencies in Table 1. Given a total of 507 contingencies sent to the BCU classifiers, the first BCU classifier dropped out 83 cases and classified them to be unstable. These 83 cases were numerically verified by the time-domain stability program. Among these cases 77 were indeed unstable according to the time-domain stability program and 6 were stable. The remaining 424 contingencies were sent to the second BCU classifier for another classification. This classifier dropped 6 cases that were classified to be stable, and they were indeed stable according to the time-domain stability program. The remaining 418 contingencies were sent to the BCU classifier III, which screened out 0 unstable cases. The remaining 418 contingencies were sent to the BCU classifier IV, which screened out 2 unstable cases. Among these contingencies, according to the time-domain stability program, 2 cases were stable. The fifth BCU classifier screened out 12 contingencies as unstable. The BCU VI classifier screened out 1 contingency, which was classified as unstable. This contingency, however, is stable, according to the time-domain stability program. The remaining contingencies entered the last BCU classifier for final classification. Among them, 378 cases were classified to be stable and all of these were verified by the time-domain stability program to be indeed stable; 25 cases were classified to be unstable. Among these cases 8 were indeed unstable and 17 were stable, as verified by the time-domain stability program. Similar explanations apply to Table 2, which summarizes the evaluation of BCU classifiers on a total of 507 contingencies on the same test system with damping effect.
2. Test system with medium loading. For the test system with medium-loading conditions, non-smooth load model, and undamped effect, we summarized the evaluation of BCU classifiers on a total of 466 contingencies in Table 3. Given a total of 466 contingencies sent to the BCU classifiers, the first BCU classifier dropped out 26 cases and classified them to be unstable. These 26 cases were numerically verified by the time-domain stability program. Among these cases 22 were indeed unstable according to the time-domain stability program and 4 were stable. The remaining 440 contingencies were sent to the second BCU classifier for another classification. This classifier dropped 8 cases, which were classified to be stable, and they were indeed stable according to the time-domain stability program. The remaining 432 contingencies were sent to the BCU classifier III, which screened out 0 unstable cases. The remaining 432 contingencies were sent to the BCU classifier IV, which screened out 4 unstable case. These 4 cases according to the time-domain stability program were stable. The fifth BCU classifier screened out 4 contingencies. Those contingencies were classified unstable. Of which, 4 contingencies were, however, all stable. The BCU VI classifier screened out 4 contingencies, which were classified as unstable. The remaining 424 contingencies were sent to the BCU classifier VI, which screened out 0 unstable cases. The remaining 424 contingencies were sent to the last BCU classifier for final classification. Among them, 419 cases were classified to be stable and all of these were verified by the time-domain stability program to be indeed stable; 5 cases were classified to be unstable. Of which, they were however all stable. Similar explanations apply to Table 4, which summarizes the evaluation

of BCU classifiers on a total of 466 contingencies on the test system with damping effect.

### Performance Evaluation

**Absolute Capture and Drop-Out.** The BCU classifiers met the requirements of absolute capture of unstable contingencies on a total of 1946 contingencies. The capture ratio (the ratio of the captured unstable contingencies to the actual contingencies) is 1.0. In other words, the BCU classifiers capture all unstable contingencies as summarized in Table 5.

**High Drop-out Stable Contingencies.** The yield of drop-out (the ratio of the dropped-out stable contingencies to the actual stable contingencies by the BCU classifiers) is 90.99% (heavy, ZIP-model, undamped), 90.58% (heavy, ZIP model, and damped), 96.17% (medium, non-smooth load model, and undamped), and 96.62% (medium, non-smooth load model, and damped), respectively, as summarized in Table 5.

**Off-Line Calculations and Robust Performance.** It should be pointed out that the same threshold values for the six BCU classifiers were applied to these 1946 cases. The computational effort required in each BCU classifier is different from each other. In addition, as the proposed BCU classifiers are connected in a sequential order, the total computational effort required to screen out a contingency (stable or unstable) by a BCU classifier is the summation of the computational effort required in each BCU classifier preceding and including the BCU classifier. For instance, the total computational effort required to screen out a contingency by the BCU classifier III is the summation of the computational effort required in BCU classifier I, II and III.

## TEPCO-BCU FOR ON-LINE TSA

TEPCO-BCU is an integrated package developed for fast and yet exact transient stability assessment (including accurate energy margin calculation and controlling UEP calculations) of large-scale power systems for on-line mode, on-line study mode, or off-line planning mode [33,63,66]. The architecture of TEPCO-BCU for on-line TSA is presented in Figure 8. Two major components exist in this architecture: a set of BCU classifiers for dynamic contingency screening and a fast and reliable time-domain transient stability simulation program and a BCU-guided time-domain method. When a new cycle of on-line TSA is warranted, a list of credible contingencies, along with information from the state estimator and topological analysis, are applied to the dynamic contingency screening program whose basic function is to screen out contingencies that are definitely stable and to screen out contingencies that are potentially unstable.

BCU classifiers screen out stable contingencies, which are then eliminated from additional analysis. BCU classifiers also screen out potentially unstable contingencies, which are sent to the fast time-domain stability analysis program, stage II of TEPCO-BCU, for final verification and, if necessary, further analysis. Thus, the slightly conservative nature of BCU method and BCU classifiers are remedied. The remaining contingencies that are undecided by BCU classifiers are then sent to the fast time-domain stability program for detailed stability analysis.

It is the ability to perform dynamic contingency screening on a large number of contingencies and to filter out a much smaller number of contingencies requiring further analysis that make on-line TSA feasible. The block function of control actions decisions determines whether timely post-fault contingency corrective actions such as automated remedial actions are feasible to steer the system away from unacceptable conditions to an acceptable operating state. If appropriate corrective actions are not available, the block function of preventive actions determines the required pre-contingency preventive controls such as real power redispatches or line switching to maintain the system stability should the contingency occur.

The algorithmic methods behind TEPCO-BCU include the BCU method [46, 47], BCU classifiers [31, 67], improved energy function construction [35], and the BCU-guide

**Table 5.** Performance evaluation of BCU classifiers on a test system with four different operating and modeling conditions: heavy, medium, ZIP load, and non-smooth load

| # | Conditions/requirements | Heavy/undamped/ ZIP load model | Heavy/damped/ ZIP load model | Medium/undamped/ non-smooth load model | Medium/damped/ non-smooth load model |
|---|---|---|---|---|---|
| 1 | Absolute capture of unstable contingencies | 100% | 100% | 100% | 100% |
| 2 | High yield of stable contingencies | 90.99% | 90.58% | 96.17% | 96.62% |
| 3 | Litile off-line computations | Yes | Yes | Yes | Yes |
| 4 | High speed | Yes | Yes | Yes | Yes |
| 5 | Robust performance | Yes | Yes | Yes | Yes |

Table 6. The average time per contingency per processor and the average time per contingency per node calculated from the total CPU time

| Number of nodes | Clock time duration | Average time per node | Number of $CPU_s$ | Average time per processor |
|---|---|---|---|---|
| 1 node | 118 seconds | 0.59 seconds | 2 CPUs | 1.18 seconds |
| 2 node | 61 second | 0.31 seconds | 4 CPUs | 1.22 seconds |

Table 7. The average time per contingency per processor/per node

| Number of CPUs | Total processing time | Average time per processor | Number of compute nodes | Average time per node |
|---|---|---|---|---|
| 2 CPUs | 211.7 seconds | 1.059 seconds | 1 node | 0.529 seconds |
| 4 CPUs | 209.3 seconds | 1.046 seconds | 2 node | 0.523 seconds |

**Table 8.** The wall clock time calculated to process 3000 contingencies, (the timings for the 1-node and the 2-node configurations are calculated for the 3000 contingencies directly from the test results)

| Number of computer nodes | Reference | Wall clock time |
|---|---|---|
| 1 node | Test results | 29.5 minutes |
| 2 node | Test results | 15.5 minutes |
| 10 nodes | Conservative estimate | 3.1 minutes |

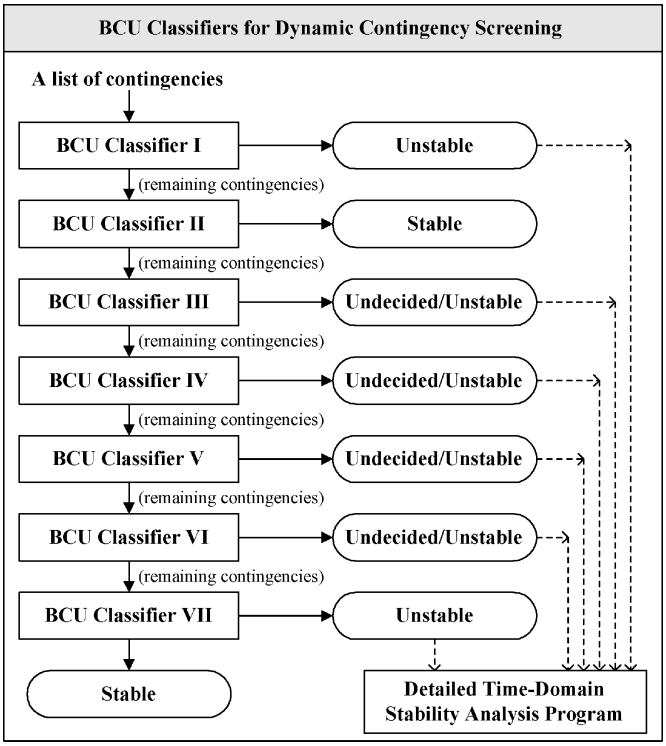


**Figure 7.** The architecture of BCU classifiers.

time domain method [33]. Several advanced numerical implementations for BCU method have been developed in TEPCO-BCU. The improved energy function construction has been developed to overcome the long-standing problem associated with the traditional numerical energy function, which has suffered from severe inaccuracy. Another distinguishing feature of TEPCO-BCU is that it provides useful information regarding derivation of preventive control against insecure contingencies and of enhancement control for critical contingencies.

The main functions of TEPCO-BCU include the following:

- Fast screening of highly stable contingencies
- Fast identification of insecure contingencies
- Fast identification of critical contingencies
- Computation of energy margin for transient stability assessment of each contingency
- BCU-based fast computation of critical clearing time of each contingency
- Contingency screening and ranking for transient stability in terms of energy margin or critical clearing time
- Detailed time-domain simulation of selected contingencies

It is true that most contingencies in a contingency list associated with a well-planned power system should be stable. Furthermore, some of these stable contingencies are highly stable in the sense of large CCTs (critical clear times). For each highly stable contingencies, one may not be very interested in its degree of stability or in its accurate energy margin other than interested in the assurance of its being indeed highly stable. On the other hand, all unstable contingencies must be all correctly identified. From an analysis viewpoint, the exact energy margin of each unstable contingency may not be important. From a control viewpoint, the exact energy margin of each unstable contingency and its sensitivity with respect to control variables can be useful for developing an effective control for preventing the system from instability should the contingency occur. As to a marginally stable or critically stable contingency, its exact energy margin provides the information regarding how far the system is away from transient instability once the contingency occurs and the sensitivity of energy margin with respect to control actions provide useful information for deriving (enhancement) control to increase the system "distance" to transient instability.

### BCU Guided Time-Domain-based Methods

The existing direct methods may not be able to compute an accurate energy function value for every contingency. The alternative is the time-domain based method for computing the energy margin. The task of how to derive an energy function value from a time-domain simulated trajectory is a practical one. Theoretically speaking, the exact energy margin is the difference between the energy value at the exit point of the original (post-fault) system and the energy value at the fault clearance point. The exit point of the original system is the intersection point between the (sustained) fault-on trajectory and the stability boundary of the (post-fault) power system. It is well known that the task of computing the exit point of the original system is very time consuming and requires several time-domain simulations. Hence, the task of computing the exact energy margin is challenging.

Given a contingency on a power system, the energy margin, an indicator for transient stability and a measure for the degree of stability/instability, for the given contingency is defined by the following formula:

$$\Delta V = V_{\mathrm{cr}} - V_{\mathrm{cl}} \tag{19}$$

where $\Delta V$ is the energy margin, $V_{\mathrm{cr}}$ is the (exact) critical energy with respect to the given fault, and $V_{\mathrm{cl}}$ is the energy at the fault clearing time. Physically speaking, the critical energy of a contingency corresponds to the total energy in-

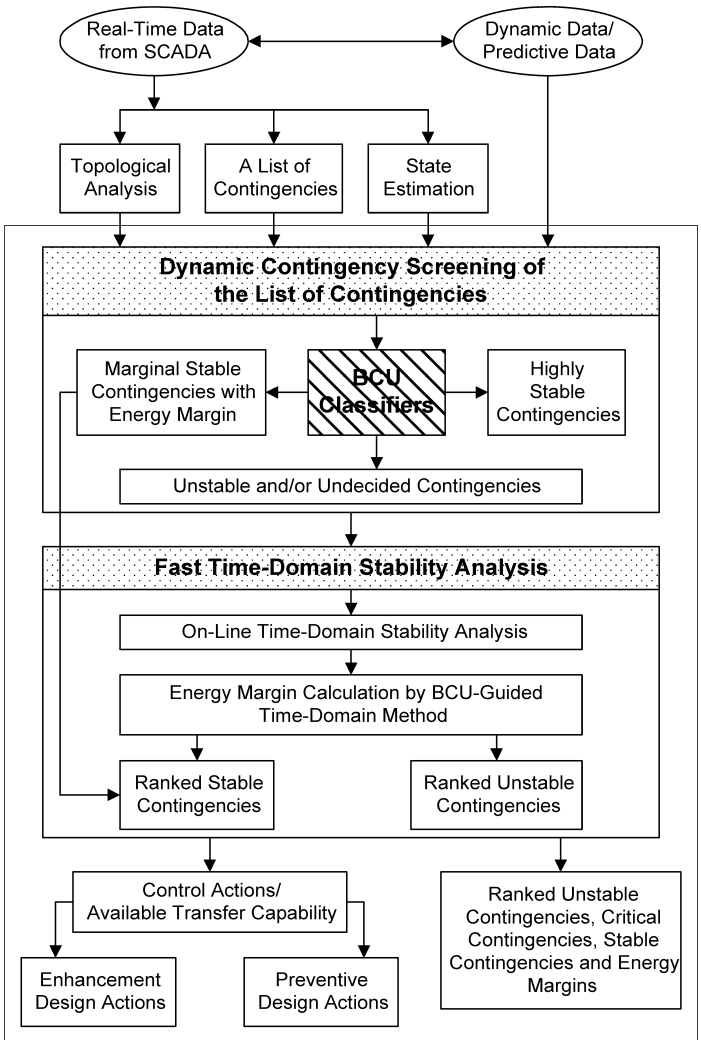


**Figure 8.** The architecture of TEPCO-BCU for on-line TSA.

jected into the fault-on system at the critical clearing time. Any attempt to develop a method for computing energy margin (19) will encounter the following difficulties

- The (exact) critical energy with respect to the given fault is very difficult to compute.
- The (functional) relationship between energy margin and fault clearing time is nonlinear and difficult to derive.

Another approach, trajectory sensitivity-based time-domain methods, has been suggested in the literature [68, 69]. It may appear from the surface that the trajectory sensitivity-based time-domain method might be faster than regular time-domain based methods. However, for a practical power system, the task of calculating trajectory sensitivity with respect to initial conditions always encounters the difficulty of formidable dimensionality explosion. This difficulty arises especially for large power system, and the trajectory sensitivity-based method is not practically applicable to energy margin computations of practical power systems. We envision that the trajectory sensitivity-based method would be useful in some applications where only moderate dimensionality explosion is involved.

A BCU-guided time-domain method for accurate energy margin calculation has been developed and tested on several practical power system models [63]. The method is reliable and yet fast for calculating energy margins whose value is compatible with that computed by the controlling UEP method. The BCU-guided time-domain method uses a BCU-guided scheme to specify, within a given time interval, a reduced-duration time interval and employs an one-dimensional search method, such as the golden bisection interpolation algorithm to the specified time interval, to reduce the total number of time-domain simulations required for finding the CCT, which is then used to compute critical energy.

The BCU-guided method is highly effective compared with existing time-domain-based methods: it is reliable and yet fast for exact stability assessment and energy margin computations. Another important property is that the energy margins computed by the BCU-guided time-domain method is comparable with, and yet less than,

exact energy margins, which are computed by an exact time-domain stability method. The effectiveness can be attributed to the fact that some information provided by the BCU method such as the exit point and the minimum gradient point are fully integrated into the BCU-guided method to significantly reduce the duration of time interval within which time-domain stability simulations are performed.

A comparison study among the BCU-guided method, the second-kick method, and the exact time-domain method in terms of accuracy and computational speed was conducted on a practical 200-bus power system model [63]. The following observations were derived from this comparison. For every contingency, the BCU-guided time-domain method always computes an energy margin that is less than, and yet close to, that computed by the exact time-domain method. This property indicates the conservativeness of the BCU-guided method in computing the energy margin. This property, which lies in the spirit of direct methods, is desirable in practical applications. A comparison between the computational speed of the BCU-guided time-domain method and that of the exact time-domain method is roughly the ratio of 1 to 2. The energy margins computed by the BCU-guided time-domain method are compatible with those computed by the exact time-domain method. Overall, the BCU-guided method has the fastest computational speed among the three methods.

### Applications to Large-Scale Test System

TEPCO-BCU program has been evaluated on a large-scale power system consisting of more than 12,000 buses and 1300 generators. In this test data, the system was modeled by a network-preserving network representation. Of the 1300 generators, 25% are classic modeled generators, whereas 75% are detail-modeled generators with an excitation system. A contingency list composed of 200 contingencies are considered. Of the 200 contingencies, 2 are unstable, about 20 are critically stable, and the remaining are stable.

The performance of TEPCO-BCU on this test system is summarized as follows. The capture of unstable contingencies by TEPCO-BCU is 100%; i.e., no unstable (single-swing or multiswing) contingencies are missed. Thus, the ratio of the number of captured unstable contingencies to the number of actual unstable contingencies is 1. The ratio of the number of stable contingencies screened out by TEPCO-BCU to the number of actual stable contingencies is about 95%. The average computation time per contingency running TEPCO-BCU on a single processor is 1.18 second for a 3.6-GHz PC.

### Parallel TEPCO-BCU

To meet the on-line dynamic contingency screening requirements for large power systems with a large number of contingencies, TEPCO-BCU needs to be implemented on a parallel processing architecture. Parallel processing is the simultaneous execution of the same task (split up and specially adapted) on multiple processors in order to obtain faster speed. The parallel nature can come from a single machine with multiple processors or multiple machines connected together to form a cluster. It is well recognized that every application function benefits from a parallel processing across a wide-range of efficiency. Some application functions are just unsuitable for parallel processing.

The test bed system is made up of two IBM 236 IBM eServer xSeries Servers interconnected by a Gigabit Ethernet Switch. The configuration for each IBM 236 eServer is as follows: CPU: Xeon 3.6 GHz – (Dual processors) with 2-MB L2 cache per Processor, Hyper-Threading Technology and Intel Extended Memory 64 Technology, 1 GB DDR II SDRAM - ECC - 400 MHz - PC2-3200, Storage Control: SCSI (Ultra320 SCSI) - PCI-X / 100 MHz (Adaptec AIC-7902), and RAM: 1 GB (installed) / 16 GB (max) - DDR II SDRAM - ECC - 400 MHz - PC2-3200.

The parallel TEPCO-BCU program has been evaluated on a large-scale power system consisting of more than 12,000 buses and 1300 generators. Of the 1300 generators, 25% are classical modeled generators whereas 75% are detail-modeled generators with an excitation system. A contingency list composed of 3000 contingencies are considered. The parallel TEPCO-BCU was run on the test data to determine the average time needed to process a contingency for each configuration tested. Two tests were ran, first using a single compute-node and then using two compute-nodes. Time was marked at the beginning of the test and again when TEPCO-BCU completed the screening to give the duration of the test, or the wall clock time. The computation performance regarding the average time per contingency per node and the average time per contingency per processor was recorded. The test showed that the parallel implementation of TEPCO-BCU cut the average processing time per node by 50% when a second compute-node was added.

Test data that were collected during the tests to record the total CPU time spent during the TEPCO-BCU run on processing of the contingencies is summarized in Tables 6–8. The average time per contingency per processor and the average time per contingency per node calculated from the total CPU time are also presented in the tables. It is observed that the average time per contingency per processor remains essentially unchanged irrespective of the number of processors given uniform testing conditions. The 2-node and 4-node test comparison is provided to observe the small degree of variation.

The timings for the 1-node and the 2-node configurations were calculated for the 3000 contingencies directly from the test results. A 5% overhead was used in the estimation of the 10-node timing, despite the fact that the testing showed overhead to be in the vicinity of 3%, in order to be on the conservative side. In addition, as the test dataset resulted in a high number of unstable and critical stable cases, it is likely that datasets that produce a more typical percentage of stable cases will result in even faster performance results for the TEPCO-BCU fast screening.

## CONCLUDING REMARKS

On-line transient stability assessment (TSA) is an essential tool needed to obtain the operating security limits at

or near real time. In addition to this important function, power system transmission open access and restructuring further reinforce the need for on-line TSA, as it is the base upon which available transfer capability, dynamic congestion management problems, and special protection systems issues can be effectively resolved. There are significant engineering and financial benefits to be expected from on-line TSA.

After decades of research and development in the energy-function-based direct methods and the time-domain simulation approach, it has become clear that the capabilities of direct methods and that of the time-domain approach complement each other. The current direction of development is to include appropriate direct methods and time-domain simulation programs within the body of overall power system stability simulation programs. For example, the direct method provides the advantages of fast computational speed and energy margins, which make it a good complement to the traditional time-domain approach. The energy margin and its functional relation to certain power system parameters form an effective complement to develop tools, such as preventive control schemes for credible contingencies that are unstable and to develop fast calculators for available transfer capability limited by transient stability. The direct method can also play an important role in the dynamic contingency screening for on-line transient stability assessment.

This chapter has presented an overview of state-of-the-art methodology and effective computational methods useful for on-line TSA. The current direction of development for on-line TSA is to combine a reliable and fast direct method and a fast time-domain method into an integrated methodology to take advantage of the merit of both methods. TEPCO-BCU has been developed under this direction by integrating the BCU method, BCU classifiers, and the BCU-guide time domain method. Several advanced numerical implementations for BCU method have been developed in TEPCO-BCU. The current version of TEPCO-BCU can perform exact stability assessment and accurate energy margin computation of each contingency of large-scale power systems. Exact stability assessment is meant to classify stable contingencies as stable and unstable contingencies as unstable, whereas accurate energy margin computation is meant to give accurate critical clearing time of each contingency of large-scale power systems. The evaluation results indicate that a parallel version of TEPCO-BCU works well with reliable transient stability assessment results and accurate energy margin calculations on a 12,000-bus test system with a contingency list of 3000 contingencies.

The group-based BCU method raises and addresses the issue of how to rigorously verify the correctness of the TSA results. In the past, this issue has been neglected because of the great computational efforts and difficulty involved. Given a credible list of contingencies, the TEPCO-BCU system can fast screen out critical contingencies. This capability in conjunction with some relevant functions can lead to several practical applications. These relevant functions include the energy function method and the controlling UEP coordinates and their sensitivities with respect to parameters or control actions. One such application is the development of a dynamic security constrained optimal power flow method. A preliminary dynamic security constrained OPF algorithm is realized based on the TEPCO-BCU engine [66]. Several applications based on TEPCO-BCU engine will be developed in the future.

As the size of power system analysis data increases due to, say, deregulation, it becomes clear that effective data-handling schemes, data verification and correction, and graphical user interface (GUI) are important for power system analysis tools. It is also clear that the approach of detailed representation for the study system and adequate and yet simplified representation for the external system is well accepted and several methods for reducing external systems have been proposed. In this regard, the data handling of the separated power system data, i.e., the data for the study system and the data for the external system, can be very complicated and error-prone with the conventional text-based format. In Ref. 70, effective data-handling schemes and GUI have been developed for an integrated power system analysis package. Two reduction techniques are also presented: one is a static reduction technique for power flow analysis, and the other is a dynamic reduction technique for transient stability analysis and small-signal analysis.

Although current power system networks cannot completely prevent disastrous cascading, their ability to manage power system disturbances can be considerably enhanced. Power systems have been relying mostly on protection systems and discrete supplementary control schemes to manage disturbance and prevent disastrous cascading. This practice needs further enhancement in both scope and depth. On-line TSA should join this practice. The design of protection systems and discrete supplementary control schemes have been often based on passive and static considerations. The parameter settings of protection systems and discrete supplementary control schemes are not adaptive to system operating conditions and network configurations. Moreover, the design and parameter settings of protection systems and discrete supplementary control schemes do not take into account system dynamic behaviors. Consequently, several adverse behaviors of protection systems and discrete supplementary control systems occur that cause service interruption of electricity and system blackouts. These behaviors include (1) unnecessary relay trippings (relays overact to stable swings) and (2) unnecessary distance relay trippings caused by system low voltage and heavy loading conditions. Increased coordination between on-line TSA and the parameter settings of protection systems and between that and discrete supplementary control schemes should help eliminate these adverse behaviors and make protection systems really adaptive.

Traditionally, an energy management system (EMS) performs generation scheduling and control of the electrical power output of generators so as to supply the continuously changing customer power demand in an economical manner. All system analysis and decision making in EMS are all based on static considerations. A linkage between EMS and protection systems, discrete supplementary control systems, and special protection systems has been missing. This linkage can be established using on-line measurements, static analysis results available at the EMS, and

additional required measurements, such as wide-area measurements, to design and develop new needed functions, both static and dynamic security, for EMS. These new functions can be utilized to develop hierachical and adaptive relays and adaptive discrete supplementary controllers and adaptive special protection systems by periodically broadcasting updated information of both static and dynamic security assessment results derived at the EMS to selected protection systems and generator sites for adaptive protection systems. This updated static and dynamic security assessment information can be used to improve the rules residing in the relays and control schemes of discrete supplementary controller and/or special protection systems so that the overall system will greatly improve the ability to manage disturbance and to prevent disastrous cascading.

## REFERENCES


1. N. Balu, T. Bertram, A. Bose, V. Brandwajn, G. Cauley, D. Curtice, A. Fouad, L. Fink, M. G. Lauby, B. Wollenberg, and J. N. Wrubel, "On-line power system security analysis (Invited paper)," *Proceedings of the IEEE*, Vol. 80, No. 2, Feb. 1992, pp. 262–280.
2. P. M. Anderson and A. A. Fouad, *Power System Stability and Control*, Second Edition, IEEE Press, 2003.
3. P. Kundur, *Power System Stability and Control*, McGraw Hill, New York, 1994.
4. P. W. Sauer and M. A. Pai, *Power System Dynamics and Stability*, Prentice-Hall, New Jersey, 1998.
5. M. Pavella, D. Ernst, and D. Ruiz-Vega, *Transient Stability of Power Systems—A Unified Approach to Assessment and Control*, Kluwer Academic Publishers, Boston, 2000.
6. A. A. Fouad and V. Vittal, *Power System Transient Stability Analysis: Using the Transient Energy Function Method*, Prentice-Hall, New Jersey, 1991.
7. B. Stott, "Power system dynamic response calculations," *Proceedings of the IEEE*, Vol. 67, 1979, pp. 219–241.
8. Electric Power Research Institute, Extended Transient/Midterm Stability Program package (ETMSP Version 3.0), Palo Alto, CA, 1992.
9. A. Kurita, H. Okubo, K. Oki, et al., "Multiple time-scale power system dynamic simulation," *IEEE Trans. Power Systems*, Vol. **8**, Feb. 1993, pp. 216–223.
10. F. P. de Mello, J. W. Feltes, T. F. Laskowski, and L. J. Oppel, "Simulating fast and slow dynamic effects in power systems," *IEEE Computer Applications in Power*, Vol. **5**, No. 3, July 1992, pp. 33–38.
11. M. Stubbe, A. Bihain, J. Deuse, and J. C. Baader, "Euro-Stag—A new unified software program for the study of the dynamic behavior of electrical power systems," *IEEE Trans. Power Systems*, Vol. **4**, Feb, 1989, pp. 129–138.
12. T. Tanaka, T. Nagao, and K. Takahashi, "Integrated analysis software for bulk power system stability," IV *Symposium of Specialists in Electric Operational and Expansion Planning*, May 23–27, 1994, Brazil.
13. P. C. Magnusson, "Transient energy method of calculating stability," *AIEE Trans.*, Vol. **66**, 1947, pp. 747–755.
14. P. D. Aylett, "The energy integral-criterion of transient stability limits of power systems," *Proceedings of IEE*, Vol. **105c**, Sept. 1958, pp. 527–536.
15. H. D. Chiang, C. C. Chu, and G. Cauley, "Direct stability analysis of electric power systems using energy functions: Theory, applications and perspective (Invited paper)," *Proceedings of the IEEE*, Vol. **83**, No. 11, Nov. 1995, pp. 1497–1529.
16. H. D. Chiang, F. F. Wu, and P. P. Varaiya, "Foundations of direct methods for power system transient stability analysis," *IEEE Trans. Circuits and Systems*, Vol. **CAS-34**, Feb. 1987, pp. 160–173.
17. H. D. Chiang, "Analytical results on the direct methods for power system transient stability analysis," in *Control and Dynamic Systems: Advances in Theory and Application*, Vol. **43**, pp. 275–334. Academic Press, New York, 1991.
18. P. P. Varaiya, F. F. Wu, and R.-L. Chen, "Direct methods for transient stability analysis of power systems: recent results," *Proceedings of the IEEE*, Vol. **73**, 1985, pp. 1703–1715.
19. F. A. Rahimi, M. G. Lauby, J. N. Wrubel, and K. L. Lee, "Evaluation of the transient energy function method for on-line dynamic security assessment,' *IEEE Trans. Power Systems*, Vol. **8**, No. 2, May, 1993, pp. 497–507.
20. H. D. Chiang, C. C. Chu, and G. Cauley, "Direct stability analysis of electric power systems using energy functions: Theory, applications and perspective (Invited paper)," *Proceedings of the IEEE*, Vol. 83, No. 11, Nov. 1995, pp. 1497–1529.
21. V. Chadalavada, V. Vittal, G. C. Ejebe, et. al., "An on-line contingency filtering scheme for dynamic security assessment," *IEEE Trans. Power Systems*, Vol. **12**, No. 1, Feb. 1997, pp. 153–161.
22. H.-D. Chiang, "Power system stability (a book chapter)," In:J. Webster G. (Ed.) *Wiley Encyclopedia of Electrical and Electronics Engineering*, John Wiley & Sons, New Yory, pp. 104–137, 1999.
23. E. G. Cate, K. Hemmaplardh, J. W. Manke, and D. P. Gelopulos, "Time frame notion and time response of the models in transient, mid-term and long -term stability programs," *IEEE Trans. Power Apparatus and Systems*, Vol. **PAS-103**, No. 1, Jan. 1984, pp. 143–151.
24. C. G. Groom, K. W. Chan, R. W. Dunn, and A. R. Daniels, "Real-time security assessment of electric power systems," *IEEE Trans. Power Systems*, Vol. **11**, No. 2, May 1996, pp. 1112–1117.
25. Y. Mansour, E. Vaahedi, A. Y. Chang, B. R. Corns, B. W. Garrett, K. Demaree, T. Athay, and K. Cheung, "B.C.Hydro's on-line transient stability assessment (TSA) model development, analysis and post-processing," *IEEE Trans. Power Systems*, Vol. **10**, Feb., 1995, pp. 241–253.
26. S. Massucco, D. Ruiz-Vega, A. Bihain, G. Burt, F. Casamatta, T. Koronides, R. Lopez, and C. Vournas, "Advance perspectives and implementation of dynamic security assessment in the open market environment," Paper 39–101, CIGRE 2002.
27. S. Massucco, L. Wehenkel, A. Bihain, D. Cirio, M. Fiorina, R. Lopez, D. Lucarella, D. Ruiz-Vega, C. Vournas, and T. Van Cutsem, "OMASES: A dynamic security assessment tool for the new market environment," *Proc. IEEE Bologna Power Tech Conf.*, June 2003.
28. K. Morison, L. Wang, and P. Kundur," Power system security assessment," *IEEE Power & Energy Magazine*, Vol. **2**, Issue 5, (Sept./Oct.) 2004.
29. L. Wang and K. Morison, "Implementation of on-line security assessment," *IEEE Power & Energy Magazine*, Vol. **4**, Issue 5, (Sept./Oct.) 2006.
30. H. D. Chiang, M. W. Hirsch, and F. F. Wu," Stability region of nonlinear autonomous dynamical systems," *IEEE Trans. Auto. Control*, Vol. **33**, Jan. 1988, pp. 16–27.
31. H. D. Chiang, C. S. Wang, and H. Li, "Development of BCU classifiers for on-line dynamic contingency screening of elec-

tric power systems," *IEEE Trans. Power Systems*, Vol. **14**, No. 2, May 1999.

32. D. Ernst, D. Ruiz-Vega, M. Pavella, P. Hirsch, and D. Sobajic, "A unified approach to transient stability contingency filtering, ranking and assessment," *IEEE Trans. PWRS*, Vol. **3**, Aug. 2001.
33. H. D. Chiang, Y. Zheng, Y. Tada, H. Okamoto, K. Koyanagi, and Y. C. Zhou, "Development of an on-line BCU dynamic contingency classifiers for practical power systems," *14th Power System Computation Conference (PSCC)*, Spain, June 24–28, 2002.
34. N. Kakimoto, Y. Ohsawa, and M. Hayashi, "Transient stability analysis of electric power system via lure-type Lyapunov function," *Trans. IEE of Japan*, Vol. **98**, 1978, pp. 566–604.
35. H. D. Chiang, "Study of the existence of energy functions for power systems with losses," *IEEE Trans. on Circuits and Systems*, Vol. **CAS-36**, 1989, pp. 1423–1429.
36. Y. Zou, M. Yin, and H. -D. Chiang, "Theoretical foundation of controlling UEP method for direct transient stability analysis of network-preserving power system models," *IEEE Trans. Circuits and Systems I: Fundamental Theory and Applications*, Vol. **50**, Oct. 2003, pp. 1324–1356.
37. C. C. Chu and H. D. Chiang, "Constructing analytical energy functions for network-preserving power system models," *Circuits Systems and Signal Processing*, Vol. **24**, No. 4, 2005, pp. 363–383.
38. A. R. Bergen and D. J. Hill, "A structure preserving model for power system stability analysis," *IEEE Trans. Power Apparatus and Systems*, Vol. **PAS-100**, 1981, pp. 25–35.
39. K. R. Padiyar and H. S. Y. Sastry, "Topological energy function analysis of stability of power systems," *Int. J. Electr. Power and Energy Syst.*, Vol. **9**, No. 1, 1987, pp. 9–16.
40. T. Athay, R. Podmore, and S. Virmani, "A practical method for the direct analysis of transient stability," *IEEE Trans. Power Apparatus and Systems*, Vol. **PAS-98**, 1979, pp. 573–584.
41. M. Hirsch and S. Smale, *Differential Equations, Dynamical Systems and Linear Algebra*. New York: Academic, 1974.
42. A. A. Fouad and S. E. Stanton, "Transient stability of a multimachine power systems. part i: pp. investigation of system trajectories," *IEEE Trans. Power Apparatus and Systems*, Vol. **PAS-100**, July 1981, pp. 3408–3414.
43. F. S. Prabhakara and A. H. El-Abiad, "A simplified determination of stability regions for Lyapunov method," *IEEE Trans. Power Apparatus and Systems*, Vol. **PAS-94**, 1975, pp. 672–689.
44. M. Ribbens-Pavella, P. G. Murthy, and J. L. Horward, "The acceleration approach to practical transient stability domain estimation in power systems," *IEEE Control and Decision Conference*, Vol. **1**, pp. 471–476, San Diego, CA, Dec. 1981.
45. R. T. Treinen, V. Vittal, and W. Klienman, "An improved technique to determine the controlling unstable equilibrium point in a power system," *IEEE Trans. Circuits and Systems-I: pp. Fundamental Theory and Applications*, Vol. **CAS-43**(4), April, 1996, pp. 313–323.
46. H. D. Chiang, "The BCU method for direct stability analysis of electric power systems: pp. theory and applications," *Systems Control Theory for Power Systems*, Vol. **64** of *IMA Volumes in Mathematics and Its Applications*, Springer-Verlag, New York, 1995, pp. 39–94.
47. H. D. Chiang, F. F. Wu, and P. P. Varaiya, "A BCU method for direct analysis of power system transient stability," *IEEE Trans. Power Systems*, Vol. **8**, No. 3, Aug. 1994, pp. 1194–1208.
48. F. A. Rahimi, M. G. Lauby, J. N. Wrubel, and K. L. Lee, "Evaluation of the transient energy function method for on-line dynamic security assessment," *IEEE Trans. Power Systems*, Vol. **8**, No. 2, May, 1993, pp. 497–507.
49. F. A. Rahimi, *Evaluation of Transient Energy Function Method Software for Dynamic Security Analysis*, Final Report RP 4000–18, EPRI, Palo Alto, CA, Dec. 1990.
50. M. A. Pai, *Energy Function Analysis for Power System Stability*, Kluwer Academic Publishers, Boston, 1989.
51. A. Llamas, J. De La Ree Lopez, L. Mili, A. G. Phadke, and J. S. Thorp, "clarifications on the BCU method for transient stability analysis," *IEEE Trans. Power Systems*, Vol. **10**, Feb. 1995, pp. 210–219.
52. G. C. Ejebe and J. Tong, "Discussion of Clarifications on the BCU method for transient stability analysis," *IEEE Trans. Power Systems*, Vol. **10**, Feb. 1995, pp. 218–219.
53. F. Paganini and B. C. Lesieutre, "A critical review of the theoretical foundations of the BCU method," *MIT Lab. Electromagnetic Electr. Syst., Tech. Rep.* **TR97-005**, July 1997.
54. F. Paganini and B. C. Lesieutre, "Generic properties, one-parameter deformations, and the BCU method," *IEEE Trans. Circuits and Systems*, Part-1, Vol. **46**, No. 6, June 1999, pp. 760–763.
55. L. F. C. Alberto, "Transient stability analysis: Studies of the BCU method; Damping Estimation Approach for Absolute Stability in SMIB Systems (In Portuguese)," *Escola de Eng. de São Carlos - Universidade de São Paulo*, 1997.
56. N. Yorino, Y. Kamei, and Y. Zoka, "A new method for transient stability assessment based on critical trajectory," *15th Power Systems Computation Conference*, Liege, Belgium, August 22–26, 2005.
57. H. D. Chiang and C. C. Chu, "Theoretical foundation of the BCU method for direct stability analysis of network-reduction power system model with small transfer conductances," *IEEE Trans. Circuits and Systems, Part I*, Vol. **CAS-42**, 1995, pp. 252–265.
58. J. Kim, *On-Line Transient Stability Calculator*, Final Report RP2206–1, EPRI, Palo Alto, CA, March 1994.
59. S. Mokhtari et al., *Analytical Methods for Contingency Selection and Ranking for Dynamic Security Assessment*, Final Report RP3103-3, EPRI, Palo Alto, CA, May 1994.
60. H.-D. Chiang and A. K. Subramanian, "BCU dynamic security assessor for practical power system models," *IEEE PES Summer Meeting*, Edmonton, Alberta, Canada, pp. 287–293, July 18–22, 1999.
61. J. Tong, H. D. Chiang, and T. P. Conneen, "A sensitivity-based BCU method for fast derivation of stability limits in electric power systems," *IEEE Trans. Power Systems*, Vol. **PWRS-8**, 1993, pp. 1418–1437.
62. D. H. Kuo and A. Bose, "A generation rescheduling method to increase the dynamics security of power systems," *IEEE Trans. Power Systems*, Vol. **PWRS-10**, 1995, pp. 68–76.
63. Y. Tada, A. Kurita, Y. C. Zhou, K. Koyanagi, H. D. Chiang, and Y. Zheng, "BCU-guided time-domain method for energy margin calculation to improve BCU-DSA system," *IEEE/PES Transmission and Distribution Conference and Exhibition*, 2002.
64. L. Riverin and A. Valette, "Automation of security assessment for hydro-Quebec's power system in short-term and real-time modes," *CIGRE-1998*, 39–103.

65. G. C. Ejebe, C. Jing, B. Gao, J. G. Waight G. Pieper, F. Jamshidian, and P. Hirsch, "On-line implementation of dynamic security assessment at northern States Power Company," *IEEE PES Summer Meeting, Edmonton*, Alberta, Canada, pp. 270–272, July 18–22, 1999.
66. Y. Tada, T. Takazawa, H. D. Chiang, H. Li, and J. Tong, "Transient stability evaluation of a 12,000-bus power system data using TEPCO-BCU," *15th Power system Computation Conference (PSCC)*, Belgium, August 24–28, 2005.
67. U.S. Patent 5,789,787, 2004.
68. I. A. Hiskens and M. A. Pai, "Trajectory sensitivity analysis of hybrid systems," *IEEE Trans. Circuits and Systems I: Fundamental Theory and Applications*, Vol. **47**, No. 2, Feb. 2000, pp. 204–220.
69. T. B. Nguyen, M. A. Pai, and I. A. Hiskens, "Sensitivity approaches for direct computation of critical parameters in a power system," *International Journal of Electrical Power and Energy Systems*, Vol. **24**, June 2002, 337–343.
70. Y. Tada, A. Ono, A. Kurita, Y. Takahara, T. Shishido, and K. Koyanagi, "Development of analysis function for separated power system data based on linear reduction techniques on integrated power system analysis package," *15th Conference of the Electric Power Supply*, Shanghai, China, Oct. 2004.

## Further Reading

T. Takazawa, Y. Tada, H.-D. Chiang, and H. Li, "Development of parallel TEPCO-BCU and BCU screening classifiers for on-line dynamic security assessment," *The 16th Conference of the Electric Power Supply Industry*, Mumbai India, Nov. 2006, 6–10.

Y. Tada, A. Kurita, M. Masuko, Y. Takahara, and K. Koyanagi, "Development of an integrated power system analysis package," *Power System Technology, 2000. Proceedings, PowerCon2000. International Conference*, Perth Australia, Dec. 2000, 4–7.

Y. Tada, T. Yamada, T. Takazawa, Y. Takahara, and T. Shishido, "Enhancement of data handling in integrated power system analysis package, named IMPACT, using information technologies," *International Power Engineering Conference*, IPEC 2003, Singapore, Nov. 2003, 26–30.

Y. Tada, A. Kurita, T. Ryuya, and H. Okamoto, "Development of voltage stability constrained OPF as one of the functions of the integrated power system analysis package, Named IMPACT," *IFAC Symposium on Power Plants & Power Systems Control*, Seoul, Korea, Sep. 2003, 15–19.

J. L. Jardim, C. S. Neto, and W. T. Kwasnicki, "Design features of a dynamic security assessment system." *IEEE Power System Conference and Exhibition*, New York, Oct. 13–16, 2004.

F. A. Rahimi, M. G. Lauby, J. N. Wrubel, and K. L. Lee, "Evaluation of the transient energy function method for on-line dynamic security assessment," *IEEE Trans. Power Systems*, Vol. **8**, No. 2, May 1993, pp. 497–507.

Electric Power Research Institute, *User's Manual for DIRECT 4.0*, EPRI TR-105886s, Palo Alto, CA, Dec. 1995.

F. A. Rahimi, *Evaluation of Transient Energy Function Method Software for Dynamic Security Analysis*, Final Report RP 4000-18, EPRI, Palo Alto, CA, Dec. 1990.

IEEE Committee Report, "Transient stability test systems for direct methods," *IEEE Trans. Power Systems*, Vol. **7**, Feb., 1992, pp. 37–43.

M. A. El-kady, C. K. Tang, V. F. Carvalho, A. A. Fouad, and V. Vittal, "Dynamic security assessment utilizing the transient energy function method," *IEEE Trans. Power Systems*, Vol. **PWRS-1**, 1986, pp. 284–291.

Dr. HSIAO-DONG CHIANG
Dr. YASUYUKI TADA
Dr. HUA LI
Cornell University, Ithaca, NY
Tokyo Electric Power Company, Tokyo, Japan
Bigwood Systems, Inc., Ithaca, NY